LEFT VENTRICULAR RESPONSE TO EXPERIMENTAL AORTIC INSUFFICIENCY: A ONE YEAR SERIAL EVALUATION

BY

RICHARD ALAN GOLDMAN

A DISSERTATION PRESENTED TO THE GRADUATE COUNCIL
OF THE UNIVERSITY OF FLORIDA IN
PARTIAL FULFILLMENT OF THE REQUIREMENT
FOR THE DEGREE OF DOCTOR OF PHILOSOPHY

UNIVERSITY OF FLORIDA
1982

ACKNOWLEDGEMENTS

It is a pleasure to acknowledge my chairman, Dr. Wilmer W. Nichols, for the opportunity to work with him at the University of Florida. I am grateful for his friendship and guidance while allowing me to pursue an independent avenue of research. I want to express my appreciation to the other committee members Drs. Daryl D. Buss, William W. Dawson, Carl J. Pepine and Wendell N. Stainsby for providing academic guidance and constructive suggestions for my graduate education and dissertation research.

I am especially grateful to several members of the Division of Cardiology, Drs. Robert L. Feldman, Edward A. Geiser, Leonard G. Christie and C. Richard Conti for their input into my research project and allowing me the opportunity to present portions of the work at national meetings.

Special thanks are due to Sharon Liberty, Linda Thompson and Dale Paley for their help in the technical aspects of this project.

I am indebted to several faculty members from Johns Hopkins, Drs. Vincent L Gott, Timothy J. Gardner, Hartzell V. Schaff, John T. Flaherty and Bernadine H. Bulkley for stimulating my interest in cardiovascular research and having confidence in my ability to perform.

Finally, I can only attempt to thank my family for their emotional support and continued confidence in me as a scientist, and more importantly, as a person.

TABLE OF CONTENTS

Abstract of Dissertation Presented to the Graduate Council
of the University of Florida in Partial Fulfillment of the
Requirements for the Degree of Doctor of Philosophy

LEFT VENTRICULAR RESPONSE TO EXPERIMENTAL AORTIC INSUFFICIENCY: A ONE YEAR SERIAL EVALUATION

By

Richard Alan Goldman

August, 1982

Chairman: Wilmer W. Nichols
Major Department: Physiology

Early and long term left ventricular responses to aortic insufficiency (AI) were investigated in eleven dogs over a one year period. Litter mate puppies were randomly separated into control (CON;N=4) and AI (N=7) groups. AI was created at four months of age by aortic leaflet perforation. Echocardiography (M-mode and two-dimensional), angiography, and hemodynamic data were obtained before and serially after AI to evaluate the left ventricular response.

Angiography showed that 5 dogs had 2+ AI, one had 3+ AI and one had 4+ AI. Angiographic estimate of the severity of AI did not change in any dog during the entire study. Computer assisted analysis of M-mode echocardiograms provided left ventricular maximum (EDD) and minimum (ESD) internal dimensions, posterior (PWT) and septal wall

thickness, shortening fraction (SF), and peak normalized rate of shortening (peak -dD/dt/D) and filling (peak +dD/dt/D). One week after creation of AI, EDD and ESD were significantly increased (33.2 ± 1.1 mm vs. 37.9 ± 0.9 mm, $p < .01$ for EDD) and then increased at a rate similar to the Controls during the rest of the study. Wall thickness increased at a significantly greater rate ($p < .04$) in the AI group when compared with the Controls (0.24 mm/mo. vs. 0.14 mm/mo., for PWT). One month after AI, shortening fraction and peak -dD/dt/D demonstrated a significant decrease (4.70 ± .51 sec^{-1} vs. 3.59 ± .30 sec^{-1}, $p < .01$ for peak -dD/dt/D) which continued to decrease throughout the study. Both angiographic and two-dimensional echocardiographic ejection fractions were decreased in the AI group. Left ventricular circumferential end diastolic and end systolic wall stresses were significantly increased three months after AI and appeared to normalize by eight months after AI.

In this experimental model of AI, early left ventricular dilatation was followed by gradual eccentric hypertrophy and a trend towards normalization of circumferential wall stress. However, left ventricular function decreased fairly rapidly after onset of AI and did not demonstrate any improvement despite left ventricular hypertrophy and normalization of wall stress.

INTRODUCTION

The problems and questions concerning volume overload of the heart and more specifically aortic insufficiency have interested investigators for the past one hundred and fifty years. Aortic insufficiency is a disease caused by the inability of the aortic valve leaflets to close properly at the end of systole thereby allowing a portion of the stroke volume to regurgitate back into the left ventricle. The heart possesses several physiological mechanisms to compensate for a chronic state of aortic insufficiency. The regurgitant volume results in dilation of the left ventricular cavity. As the left ventricle dilates, its ability to maintain an adequate forward stroke volume and cardiac output is predicted from Starling's law of the heart relating stroke volume to myocardial fiber length. Secondly, left ventricular dilation may result in an increase in left ventricular wall tension. This can be inferred from the Laplace equation, $T=P \cdot r/2h$, which states that wall tension of a sphere is equal to the internal pressure multiplied by the radius of the sphere divided by twice the wall thickness. The increase in left ventricular wall tension may be a stimulus for an increased rate of growth of left ventricular muscle. This increase in size and thickness of the left ventricle, known as left ventricular hypertrophy, should reduce the tension placed on the left ventricular wall per unit muscle mass or fiber. Thirdly, there is an increase in inotropic support of the heart as supplied by endogenous levels of

circulating catecholamines and direct stimulation of cardiac sympathetic fibers. Sympathetically mediated enhancement of fiber shortening should help to maintain an adequate forward cardiac output.

Because these compensatory mechanisms are so adequate, chronic aortic insufficiency characteristically is often well tolerated for many years until symptoms develop. As more physiologic techniques evolved for myocardial protection during valve replacement, it has become apparent that deleterious and often irreversible damage to the heart may occur despite technically adequate aortic valve replacement. Thus, our understanding of this disease process and its compensations are incomplete. Therefore, attention has been directed towards developing sensitive and reliable physiologic techniques for evaluation of left ventricular function and predicting the functional consequences of aortic insufficiency during the asymptomatic phase. The possibility that irreversible myocardial damage may occur before evidence for heart failure appears emphasizes the need for a more complete understanding of the timing and sequential physiologic changes that occur during aortic insufficiency.

There are several problems involved in evaluating the physiologic changes associated with aortic insufficiency in humans. Onset of the disease is frequently unknown because patients remain asymptomatic for many years. Aortic insufficiency is often associated with other valvular lesions such as aortic stenosis or mitral insufficiency. Compensatory processes associated with aortic insufficiency may be markedly variable in humans because of the influence of age, hypertension or other diseases. Since it is difficult to evaluate the pure, isolated

lesion of aortic insufficiency of known duration in humans without any influence of other cardiac or non-cardiac diseases, a more critical physiologic assessment of aortic insufficiency may be accomplished using an experimental model.

Previous Studies

Although Hodgkin was the first to give a clinical description of this disease (1), it was D.J. Corrigan who three years later attempted to explain the clinical findings of aortic insufficiency (2). Corrigan's recognition of the importance of regurgitation is apparent in the following description from his paper.

> The duration of this disease is very uncertain. No case was of less duration than two or three years and some of the cases at present under treatment have been of seven or eight years standing. The time during which the disease may continue without terminating fatally, seems to depend principally upon the extent to which regurgitation is permitted. (2, p.234)

His understanding of factors contributing to the severity of the disease can best be appreciated from his original statement.

> The danger of the disease is in proportion to the quantity of blood that regurgitates, and the quantity that regurgitates will be large in proportion to the degree of inadequacy of the valves, and to the length of pause between the contractions of the ventricle during which blood can be pouring back. (2, p.241)

Many present day hypotheses concerning factors contributing to the severity of aortic insufficiency can be traced to Corrigan's paper.

Even though there was some experimental work done by German investigators in the late 19th century concerning changes in blood pressure in acute aortic insufficiency, it was not until Stewart's thesis was published in 1908 that effects of aortic insufficiency on the heart and

characteristics of systolic ejection were examined in detail (3). Stewart used an instrument known as a MacCallum valvulotome (4), inserted via the left carotid artery to tear an aortic valve leaflet to produce experimental aortic insufficiency in dogs. In the ten out of thirty experiments which were successful, he determined that aortic insufficiency "barely" increased systolic output and that regurgitant volume was negligible. He reasoned that the flow into the ventricle during diastole is determined by the size of the opening as well as the aortic to left ventricular pressure gradient. End systolic pressure measured at the dicrotic notch of the aortic pressure waveform was approximately 15 mm Hg above end diastolic pressure. Since the aortic leak was small as compared with the mitral orifice, he reasoned that a major portion of diastolic left ventricular filling occurred through the latter. He also concluded that the decrease in arterial diastolic pressure was due to "runoff" of blood flow through capillaries and not due to regurgitation.

Three years later, Stewart reported on the gross pathologic findings of the heart after experimentally induced aortic insufficiency (5). He observed that left ventricular hypertrophy developed within one week after creation of aortic insufficiency. He concluded that the hypertrophy was the result of an increased workload needed to maintain diastolic tension and resist left ventricular dilation. Several other investigators reported detection of left ventricular hypertrophy (6-8) with aortic insufficiency, although initial detection of hypertrophy and whether or not hypertrophy preceded left ventricular dilatation were variable.

Wiggers conducted similar investigations into acute experimental aortic insufficiency (9,10) and concluded that regurgitation of pressure and not volume during diastole created the "collapsing" pulse pressure. "Regurgitation of pressure" into the ventricle was based upon observations of a decrease in diastolic pressure (left ventricular volume was not measured) during the cardiac cycle after aortic insufficiency was induced. A similar fall in aortic diastolic pressure was observed even after administration of nitroglycerin or epinephrine. Therefore, the change in diastolic pressure appeared independent of peripheral vessel vasomotor tone. He hypothesized that "regurgitation of pressure" should increase initial tension within the ventricle. A tracing of the intraventricular pressure during aortic insufficiency did not appear to show an elevated end diastolic pressure. He concluded that both the increased rate of rise and absolute magnitude of ventricular pressure observed during systole may be due to higher initial tension within the ventricle. This was referred to as "the dynamic law of the ventricle" as demonstrated in separate preparations by Frank, Starling, and Wiggers. Much of the dispute over whether there was an important regurgitation of blood volume back into the left ventricle centered around the ability to accurately measure left ventricular volume. Wiggers contended (10) that Stewart's use of the cardiometer or MacCallum's plethysmograph technique (11) did not distinguish between left and right ventricular volumes. Investigators who evaluated left ventricular volume from an X-ray shadow included Bazett and Sands and Wiggers et al. (7,12). These studies were reevaluated by Wiggers (13) a year later, and he criticized this technique because an increase in heart rate tended to decrease left

ventricular diastolic size. Also anterior-posterior enlargement could not be clearly distinguished and considerable changes in volume were required for detection by these X-ray techniques.

During this period of time, other evidence was accumulating which supported the hypothesis that an important volume regurgitated into the left ventricle during aortic insufficiency. MacCallum (11) used a cardiac plethysmograph in 1911 to measure volume excursions. He was one of the earliest proponents of the predominant role of regurgitant volume in the pathophysiologic processes observed with aortic insufficiency. Lewis and Drury (14) reported cardiac enlargement in five patients with arteriovenous fistulas and commented on reports of French surgeons who corrected fistulas and observed an immediate postoperative decrease in ventricular size. Dock and O'Hara (15) were the first investigators to report aortic blood flow measured directly during aortic insufficiency using an aortic haemodromograph. They demonstrated that aortic valve leaflet destruction caused definite back flow. Gladstone (16) described a theoretical analysis of aortic insufficiency based on principles of flow and pressure which supported the original conclusions of MacCallum. By 1931, evidence had accumulated to support the hypothesis that the regurgitant volume played a significant role in the hemodynamic changes which occurred in aortic insufficiency. Wiggers, convinced by mounting evidence that the regurgitant flow was important, examined hemodynamic changes during acute aortic insufficiency. He concluded that the size of leak, but not the duration is critical in determining the amount and percent regurgitant flow into the ventricle (17). Furthermore, he postulated that gradations of regurgitant flow

might correlate well with the clinical appearance of the patient ranging from the asymptomatic to congestive heart failure stages (13).

After a twenty year period where no important contributions concerning aortic insufficiency were published, a variety of new indirect and direct techniques were developed for estimation of the magnitude of regurgitant flow. These techniques included indicator-dilution (18-21), contrast angiocardiography (22-24), and the electromagnetic flowmeter (25-33). Since introduction of upstream sampling technique for quantitating valvular regurgitation was described by Wood et al. (18), regurgitant flows ranging between 30-70% of total forward stroke volume have been reported (19). Sandler et al. (22) determined total left ventricular stroke volume by calculating the volume of the left ventricular cavity during both end diastole and end systole using biplane angiocardiograms. Regurgitant volume was then calculated by subtracting net forward volume determined by the Fick method from total stroke volume. After development of the square-wave electromagnetic flowmeter by Denison, Spencer and Green (34), several groups reported characteristics of regurgitant flow in experimental animals (25-30) and in patients undergoing valve replacement surgery (31-33). Morrow et al. (31) reported that regurgitant fraction ranged from 63-75% in eight patients undergoing valve replacement due to aortic insufficiency. A later study by the same group (32) demonstrated that regurgitant flow rate remained unchanged even when heart rate increased from 50 to 170 bpm in six patients. More recently, techniques such as radionuclide angiography (35-37) and insertion of catheter-tip velocity transducers (38-39) have also been used

to estimate the regurgitant fraction in patients with aortic insufficiency. These newer techniques have confirmed that regurgitant fractions ranging from 70-75% may exist in some patients with severe aortic regurgitation. All these techniques which estimated magnitude of the regurgitant volume have emphasized the importance of volume overload when evaluating left ventricular adaptations to aortic insufficiency.

Effects of aortic insufficiency on coronary blood flow were first reported in 1926 by Smith et al. (40). They collected coronary sinus flow and observed that the decrease in coronary sinus blood flow correlated well with the decrease in aortic diastolic pressure. Ten years later, Green (41) noted that while there was only a decrease in coronary blood flow during diastole, a concomitant increase occurred during systole. The resultant total coronary blood flow was thus dependent upon both coronary vascular resistance and mean arterial pressure. Effects of aortic insufficiency on coronary blood flow were reevaluated more than twenty years later, when two separate studies demonstrated an increase in coronary flow with aortic insufficiency (42,43). Both of these studies suggested that the increase in cardiac work necessary to maintain a normal forward cardiac output should result in a decrease in coronary vascular resistance. This decrease in coronary resistance was greater than the decrease, if any, in aortic diastolic pressure, thereby increasing coronary flow.

More recently, several studies have reported that the transmural distribution of coronary blood flow is altered in experimental animals with acute aortic insufficiency (44,45). Falsetti et al. (45) demonstrated that subendocardial perfusion decreased even though total

coronary blood flow increased. Feldman et al. (46) have suggested that coronary blood flow reserve, defined as the peak flow response to a transient coronary occlusion, is decreased in experimental animals with acute aortic insufficiency. The precise physiologic importance of coronary hemodynamic changes associated with aortic insufficiency remain to be investigated.

There was also considerable interest in the hemodynamic alterations occurring in aortic insufficiency. The most common approach used to study hemodynamic effects of this lesion was to assess changes in left ventricular and systemic pressures, ventricular volume and cardiac output. Two separate studies using different experimental models demonstrated that acute aortic insufficiency produced a decrease in forward cardiac output, and an increase in both systemic vascular resistance and left ventricular end diastolic pressure (26,29). There was a marked downward and rightward shift in the left ventricular function curve (26). Another study which stressed the importance of volume overload in aortic insufficiency demonstrated that infusion of saline in dogs with arteriovenous fistulas increased end diastolic pressure, but not left ventricular stroke work (47). Brockman (48) demonstrated a descending portion of the left ventricular function curve in their experimental model.

Although these studies evaluated the pump function of the left ventricle with a volume overload, they provided little insight into either the mechanisms responsible for these changes or the consequences induced by this overload on the myocardium. Furthermore, these studies did not distinguish between effects of altered load on the

myocardium and the possibility of an alteration in the intrinsic contractile state of the myocardium. An evaluation of myocardial contractility based on the principles of isolated muscle mechanics should consider the interaction of preload, afterload, and inotropic state of the myocardium. Urschel et al. (49) used a model of acute and reversible aortic insufficiency and compared tension-velocity curves obtained during AI to a control period at the same end diastolic volume. They demonstrated that contractility as defined by Vmax was unchanged during aortic insufficiency in this model. Furthermore, they concluded that this unaltered contractile state might be attributed to reduction in impedance to left ventricular ejection. Gault et al. (50) also evaluated contractility by constructing tension-velocity curves from measurements made in five patients before and after valve replacement for aortic insufficiency. They found that in patients with depressed preoperative myocardial contractile state, there was no post-operative improvement in contractility despite a reduction of myocardial wall tension to the normal range. Postoperative improvement in cardiac index was associated with the reduction of the regurgitant volume and related changes resulting in an increase in the forward stroke volume. Several more recent investigations have used various physiologic techniques in an attempt to quantify contractility. These studies have suggested that contractility may be increased (51,52) in acute aortic insufficiency, and either normal (53-56) or decreased (57-60) in chronic aortic insufficiency. Thus, due to conflicting evidence, definitive conclusions about the contractile state of the myocardium associated with aortic insufficiency cannot be made.

The Present Study

The objective of this research was to serially evaluate the acute and long term left ventricular adaptations to a volume overload created in an experimental model of aortic insufficiency. Serial M-mode echocardiography was selected as an adequate non-invasive method to simultaneously assess alterations in left ventricular dimensions, wall thickness and contractile function in the conscious animal. The combination of serial echocardiographic measurements along with angiographic measurements and hemodynamic data to evaluate the physiologic sequence of left ventricular responses to experimentally induced aortic insufficiency during a one year period has not been previously reported.

A major hypothesis of this research was that left ventricular function remained normal during both acute and chronic phases of aortic insufficiency. In view of this hypothesis, it was important to determine the timing and sequence of the left ventricular response to aortic insufficiency. Despite its limitations, this study provided original and important information concerning the left ventricular responses of aortic insufficiency in a conscious animal model because (1) the severity of experimentally induced aortic insufficiency was known throughout the study period, (2) the entire duration of aortic insufficiency was known, (3) the study was relatively non-invasive and the pericardium remained intact, and (4) the study was designed to compare the left ventricular responses of purebred litter mate animals randomized to an experimental and a control group. Although there are

many differences between this experimental model and aortic insufficiency observed in humans, this study may provide valuable information in understanding some of the physiologic processes which occur during the development of the human disease.

METHODS

Experimental Animals

Purebred litter mate foxhounds were selected as the experimental animal for this study. This selection was made for several reasons. Dogs were chosen because they are an easily trainable animal and the physiologic changes which occur at an accelerated rate during aortic insufficiency may closely parallel the human disease. Purebred litter mate animals were chosen to minimize variability in the animals' growth pattern. The foxhound breed was selected because prior experience with this species indicated that a very high percentage of these dogs would be easily trainable. It was critically important for the non-invasive cardiac assessment that these dogs be relaxed and responsive.

Fourteen purebred litter mate foxhound puppies were randomly separated into a control group (Con; N=4) and an aortic insufficiency group (AI; N=10). These dogs were obtained at two months of age. They underwent two months of behavioral training and adjustment to the lab before satisfactory non-invasive assessment of the heart using M-mode echocardiography could be performed.

Creation of AI

At approximately four months of age, each AI group dog underwent a cardiac catheterization using sodium pentobarbital (25 mg/kg) anesthesia. Under fluoroscopic guidance, a 7 French catheter was introduced via the right carotid artery and positioned at the aortic valve. A Bing stylet was inserted into the catheter and one of the valve leaflets was perforated either once or twice (Figure 1). The defect was enlarged by inserting a flexible metal basket catheter (Figure 2) through the leaflet perforation into the left ventricle. The basket was "opened" and withdrawn through the perforation (Figure 2). Three animals died during this procedure due to technical difficulties. The remaining seven dogs tolerated the procedure well and comprised the AI group (N=7).

Aortic Angiography

The basket catheter was replaced with an angiographic catheter which was advanced to the ascending aorta. An aortogram was filmed on the AI group to estimate the magnitude of aortic insufficiency created using a standard angiographic technique (61). Severity of valvular insufficiency can be assessed angiographically by observing the degree of opacification of the left ventricle following rapid hand injection of 3-5 cc. of Renografin 76 into the proximal aorta. Estimation of the magnitude of AI was based on degree of left ventricular opacification. Severity of AI determined angiographically was quantified as follows:

Figure 1. This photograph of an aortic valve demonstrates a perforation created in this study after twenty months. The pointer is positioned through the aortic valve perforation.

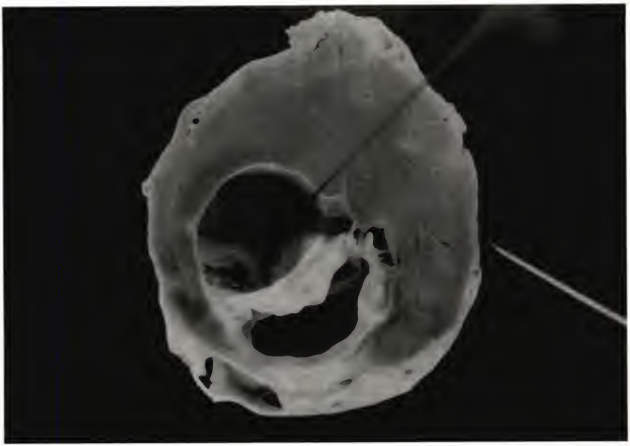

Figure 2. A Bing stylet was used to perforate the aortic valve and a flexible metal basket catheter was used to enlarge the lesion.

BING STYLET

BASKET CATHETER

1+, only a regurgitant jet; 2+, regurgitant jet and faint opacification of the left ventricle; 3+, dense opacification of the left ventricle; and 4+, the left ventricular opacification more dense than the aortic (Figures 3,4).

Repeat aortograms were performed on the AI group at seven and twelve months of age to confirm that the defect remained patent and to assess the magnitude of AI (Table 1). Aortograms were also done on the control group at twelve months of age to establish that these dogs had competent aortic valves.

M-Mode Echo Techniques

The principles of ultrasound upon which M-mode and two-dimensional echocardiographic techniques are based are presented in the Appendix. M-mode echocardiograms were obtained in the AI group at four months of age (the week preceding the creation of AI), approximately one week later and at monthly intervals between four and sixteen months of age (Table 1). Control group echocardiograms were obtained at four months of age and then at monthly intervals between six and sixteen months of age. Echocardiograms were obtained with the dogs in a conscious, relaxed state, standing upright without restraints. A 3.5 MHz echo transducer interfaced with an Irex 101 Continutrace recorder and multichannel strip chart recorder were used to record standard limb lead electrocardiographic and simultaneous left ventricular echocardiographic tracings at 50 and 100 mm/sec. On each dog, the echo transducer was placed on the right lateral chest wall, in either the

Figure 3. This sequence of four angiographic frames, from bottom to top, demonstrate the lesion created by perforation of the aortic valve.

Figure 4. Angiographic estimate of the magnitude of AI in this aortic root angiogram in 2+ AI.

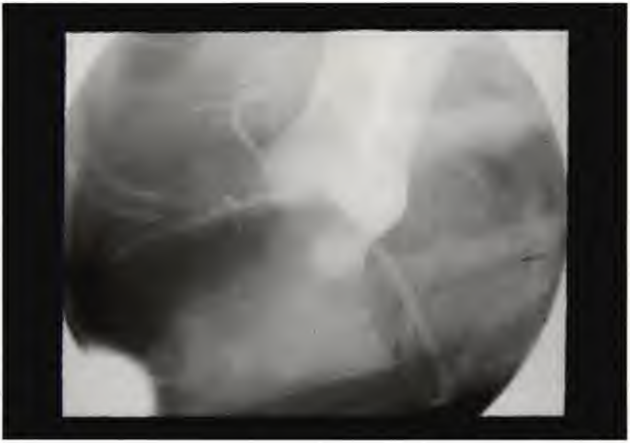

TABLE 1
SERIAL DATA COLLECTION

Controls (N=4); AI (N=7)

	0	1	2	3	4	5	6	7	8	9	10	11	12	13	14	15	16
Angiographic					X			X					X				
Hemodynamic					X			X					X				
Echocardiographic				X	X	X	X	X	X	X	X	X	X	X	X	X	X
					† AI												

third or fourth intercostal space near the mid axillary line, and the left ventricle scanned from the aortic root to apex until a reproducible echocardiogram at the minor axis was obtained just below the level of the mitral valve. Figure 5 is an illustration of M-mode echoes obtained on a Control and AI dog at four, six, ten and sixteen months of age.

Three to five consecutive cardiac cycles from each M-mode echocardiogram were selected for analysis on the basis of clear endocardial border resolution and apposition of septal and posterior wall motion. These selected M-mode echocardiograph recordings were placed on a digitizing pad (HP9874A) and right septal, left septal, posterior endocardial and posterior epicardial borders were traced. Digitized borders were converted to a series of digital coordinates representing the position of these borders throughout the cardiac cycle. In order to record accurately motion of cardiac structures, it is necessary for the digitizing procedure to have an adequate frequency response. Upton and Gibson have demonstrated from Fourier analysis of left ventricular wall movement that 90% of the total movement is present at frequencies of 10 Hz or less (62). Since the digitizing procedure of the present study was developed from algorithms used in Upton and Gibson's report, the frequency response was assumed to be similar. Each digital border in the present study was reduced to a curve consisting of equally spaced points at 10 msec intervals (100/sec) from the onset of the QRS complex of the cycle studied. In addition, calibration information, representing a time interval (1 sec) and depth (5 cm), were digitized. Trace orientation on the digitizing

Figure 5. These M-mode echocardiograms demonstrate the change in left ventricular internal dimensions and wall motion in a control and AI dog at four (before AI), six, ten and sixteen months of age.

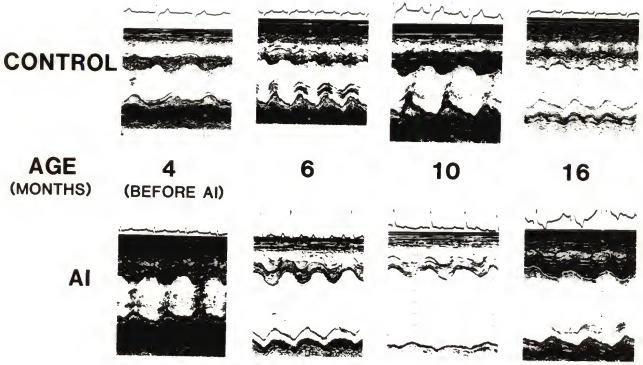
CONTROL
AGE
(MONTHS)
4
(BEFORE AI)
6
10
16
AI

table can be established since time and depth calibrations must be perpendicular to each other. End diastolic dimension was calculated as the difference between the initial points in the left septal and posterior endocardial wall borders at the Q wave of the electrocardiogram. End systolic dimension was taken as the minimum diameter during the cardiac cycle. Wall thickness was calculated as the difference between initial points on the septal and posterior wall wall borders respectively, i.e. at the Q wave. The R/h ratio was calculated as

$$R/h = \frac{\text{(end diastolic dimension/2)}}{\text{LV posterior wall thickness}}.$$

Shortening fraction was calculated as

$$SF = \frac{\text{(end diastolic dimension - end systolic dimension)}}{\text{end diastolic dimension}}.$$

The normalized rate of change in dimension was calculated as

$$dD/dt/D = \frac{[Dn+1 - Dn \text{ (mm)}]}{.010 \text{ sec}} / Dn(\text{mm}).$$

This calculation describes a rate of dimension change, positive (+) or negative (-), normalized for the instantaneous ventricular dimension. This normalization procedure was done to permit comparison of filling and emptying patterns in ventricles of different size. The comparison is valid if it is assumed that the rate of dimension change is a linear function of dimension over the range of left ventricular dimension evaluated in this study. Computations were carried out using a free standing graphics terminal (HP2647A) and hard copy of the results obtained in both printed and plotted form (HP Plotter Printer 7245A; Figure 6).

Figure 6. (Left) Computer tracing of the digitized echocardiographic borders. AEND (right ventricular endocardium); RSEP (right septal); LSEP (left septal); PEND (left ventricular posterior endocardium); PEPI (left ventricular posterior epicardium); 57.7 mm is the end diastolic dimension; 40.5 mm is the end systolic dimension. (Top Right) Computer tracing of the change in LV (left ventricular) dimension during the cardiac cycle. (Bottom Right) Computer tracing of D DIM/DT/DIM (normalized rate of dimension change) during the cardiac cycle. The equation for calculation of dD/dt/D is shown in the bottom panel.

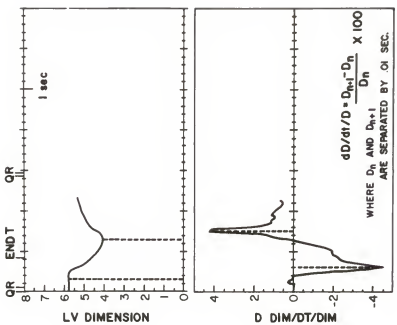
QR
END T
QR
1 sec
LV DIMENSION
D DIM/DT/DIM
dD/dt/D = Dn+1 - Dn / Dn X 100
WHERE Dn AND Dn+1 ARE SEPARATED BY .01 SEC.

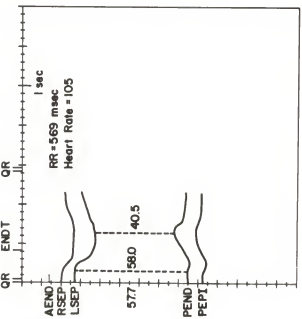
QR
END T
QR
1 sec
RR = 569 msec
Heart Rate = 105
AEND
RSEP
LSEP
577
580
40.5
PEND
PEPT

Two Dimensional Echo Techniques

Two dimensional (2D) echocardiograms were obtained on both AI and control groups at twenty-four months of age. Similar to the M-mode echoes, the 2D echocardiograms were recorded while the dogs were in a conscious, comfortable state and standing upright. A Diasonics V-3400 R ultrasonograph connected to a 3.5 MHz phased array transducer and recorded on a Scotch L-500 video cassette were used to record simultaneous left ventricular echocardiographic images and electrocardiographic tracings. On each dog, the phased array echo transducer was placed on the right lateral chest wall, in either the third or fourth intercostal space, and the left ventricle scanned until a high quality reproducible cross-sectional echogram at the minor axis was obtained just below the level of the mitral valve. The echo transducer was then rotated ninety degrees and the left ventricle scanned until an adequate image of the parasternal long axis from apex to aortic root was obtained and recorded (Figure 7).

These 2D echocardiograms were reviewed and photographs from end diastolic and end systolic frames of both cross-sectional and long-axis views of each dog were obtained. From these photographs, endocardial and epicardial borders were manually traced. These 2D tracings were then placed on a digitizing pad (HP9874A) and the endocardial and epicardial borders were digitized. Digitized borders were converted to a series of digital coordinates representing position of these borders similar to the M-mode echo tracings, but only for end diastolic and end

Figure 7. This example demonstrates the anatomical slice and corresponding 2D echocardiogram obtained from one dog with 2+ AI at twenty-four months of age.

CROSS SECTION

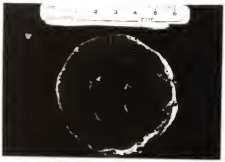

LONG AXIS

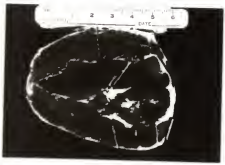

systolic frames. Calibration information representing a depth interval of 5 cm was also digitized.

Left ventricular volume was calculated using a modification of the method described by Dodge et al. (63) for biplane angiograms. The left ventricular chamber was assumed to be ellipsoidal in shape for the purpose of calculating its volume (Volume = $4\pi abc/3$, where c is the major semiaxes, and a and b are respective minor semiaxes). The minor diameter (D) was derived from the planimetered area (A) of the left ventricular endocardial outline as follows:

$$A = \frac{\pi DL}{4} \quad (1a)$$

$$D = \frac{4A}{\pi L} \quad (1b)$$

$$D/2 = \frac{2A}{\pi L} \quad (1c)$$

where L is the long axis of the left ventricular chamber measured directly from the digitized echo and D/2 is the minor semiaxes calculated from both the cross-section and long axis echoes. It is important to note that the long axis measured is not an anatomic axis, but rather the longest length calculated from the digitized echo. Therefore, the expression for volume becomes

$$V = \frac{4}{3} \pi \frac{(2A)cs}{(\pi L)cs} \frac{(2A)La}{(\pi L)La} \frac{(L)La}{(2)} \quad (2a)$$

$$V = \frac{8}{3\pi} \cdot \frac{(A)cs \cdot (A)La}{Lcs} \quad (2b)$$

where Acs and Lcs are the planimetered area and the longest measured axis of the cross-sectional echo, respectively; and (A)La and (L)La are the planimetered area and longest measured axis of the long axis echo.

Left ventricular muscle mass was calculated from the difference between the left ventricular epicardial and endocardial outlines as follows:

LV Mass = (LV epicardial volume - LV endocardial volume) x 1.05 (3)

where 1.05 is the specific gravity for muscle (64-66).

Left Ventricular Angiography

Left ventricular (LV) angiograms were filmed approximately 10-20 minutes after aortic root angiography with the anesthetized dog in an 80° right anterior oblique (RAO) position. In the AI group angiograms were done during the initial catheterization at four months of age and then repeated at seven and twelve months of age (Table 1). LV angiograms were obtained on the control group dogs at twelve months of age. These angiograms were obtained by positioning the same catheter which was used to film the aortic angiograms into the left ventricular chamber. Radiopaque contrast media (Renografin 76) was manually injected and the left ventricular chamber was filmed for several beats without electrocardiographic evidence of arrythmias. LV angiograms and a calibration grid used to standardize the depth of the level of the heart from the film were recorded on cine angiographic film.

The developed angiographic films were projected onto the screen of a Vanguard XR-35 projector. The outline of the opacified left ventricle obtained from the frame immediately preceding the onset of systole (the onset of left ventricular contraction) was traced and considered the end diastolic frame and the one immediately preceding

the opening of the mitral valve was traced and considered the end systolic frame. These LV angiographic tracings were digitized using techniques similar to those previously described in the M-mode and 2D echo technique sections. Computer analysis of the digitized angiograms provided the planimetered area of the LV outline, maximum length of the LV outline and transverse diameter which bisected and was perpendicular to the maximum length. Figures 8 and 9 illustrate left ventricular angiographic tracings in end diastole and end systole from a dog with 2+ AI and another with 4+ AI.

Left ventricular volumes were calculated using methods described by Dodge et al. and Sandler and Dodge (67,68) and Greene et al. (69) for single plane angiograms. The method of Dodge calculates LV volume as

$$V = \frac{\pi}{6} K^3 L D^2 \qquad (4)$$

where V is the calculated LV volume in cm^3, corrected for x-ray magnification; K is the correction factor for x-ray magnification; L is the measured maximum length of the LV in cm, represented in all dogs by the distance from the apex to the point of intersection of the mitral valve and the left sinus of Valsalva; and D is the calculated minor axis in cm obtained from equation (1b) as described in the previous section on volume determination from 2D echo techniques.

The method of Greene calculates the LV volume as

$$V = \frac{\pi K^3 L M^2}{6} \qquad (5)$$

where M is the minor axis, in cm, measured as the transverse axis of the LV outline, perpendicular to and bisecting the maximum length, L. Greene defines the maximum length, L, as the distance from the apex to

Figure 8. Sequence of digitized tracings of LV angiograms in end diastole and end systole. Control LV angiogram was filmed at four months of age right before creation of AI.

2+ AI

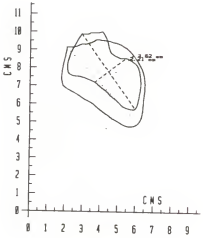

CONTROL

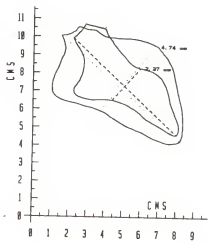

3 MOS. POST AI

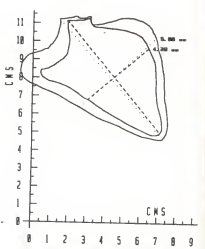

8 MOS. POST AI

Figure 9. Digitized tracings of LV angiograms in end diastole and end systole. Control LV angiogram was filmed at four months of age right before creation of AI.

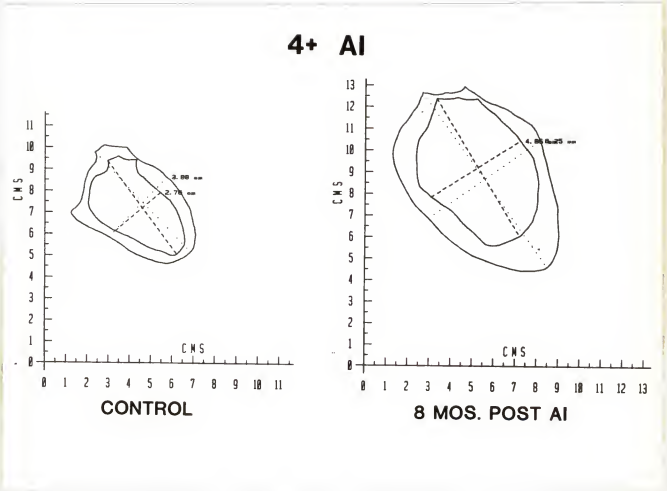
4+ AI
CMS
CMS
CONTROL
CMS
CMS
8 MOS. POST AI

the midpoint of the left atrial outline. Although Dodge and Greene define L slightly differently, the two L's are coincident in the RAO projection (70). Regression equations derived from Bentivoglio's study of volume determinations in LV casts of dogs (70,71) were performed on both the Dodge and Greene calculations as follows:

$$\text{Dodge:} \quad y = 0.91x - 1.97 \qquad (6a)$$

$$\text{Greene:} \quad y = 0.78x + 2.60 \qquad (6b)$$

where y is the LV volume in cm^3, corrected for the biased overestimation characteristic of each method; and x is the calculated volume from the Dodge and Greene equations. Ejection fraction (EF), calculated as

$$EF = \frac{(EDV - ESV)}{EDV} \times 100 \qquad (7)$$

was determined for both the calculated Dodge and Greene equations and also for corrected volumes computed from the regression equations.

Left Ventricular Wall Stress

Combined angiographic and LV pressure recordings were obtained on the AI group at four, seven, and twelve months of age for calculation of LV circumferential wall stress (Table 1). These data were also collected on the Control group at twelve months of age in order to establish normal values for wall stress in these animals at this age.

LV angiograms were obtained on these anesthetized dogs as described in the previous section. Angiographic data necessary for the calculation of circumferential wall stress were the long axis radius

(a), short axis radius (b), and the wall thickness (h) obtained at the level of the short axis. Computer analysis of the digitized angiograms provided the planimetered area of the LV cavity and long axis. This was taken as the distance from apex to the point of intersection of mitral valve and left sinus of Valsalva. The short axis was derived from the Dodge equation (1b) which uses the planimetered area of the LV outline as previously described (LV angiography). Wall thickness was measured approximately at the level of the short axis as the difference between LV endocardial outline and cardiac silhouette.

Recordings of LV and aortic pressure were obtained by insertion of a multisensor high-fidelity Millar micromanometer into the left ventricle via the right or left carotid artery (72,73). In addition, a simultaneous electrocardiographic recording was obtained. LV end diastolic pressure (LVEDP) was measured at the onset of the QRS complex and LV end systolic pressure (LVESP) was obtained at the dicrotic notch of the aortic pressure waveform.

Calculations of LV circumferential end diastolic and end systolic wall stress were obtained from these anesthetized dogs using four sets of equations (74-77). The different models on which these equations are based make different assumptions about the left ventricular geometry and the distribution of stress across the ventricular wall. Table 2 lists the equations used to calculate LV wall stress in terms of g/cm^2. These equations were programmed onto a HP 9820A calculator where the stress calculations were performed.

TABLE 2
EQUATIONS FOR CALCULATION OF LV CIRCUMFERENTIAL WALL STRESS

Model	Author(s)	Equation	
Thin-Walled Sphere	Laplace	$\sigma = \frac{Pr}{2h}$	(8a)
Thin-Walled Ellipsoid	Sandler and Dodge	$\sigma = \frac{Pb}{h}\left(1 - \frac{b^3}{a^2(2b+h)}\right)$	(8b)
Thin-Walled Ellipsoid	Falsetti et al.	$\sigma = \frac{Pb}{h}\left(\frac{2a^2-b^2}{2a^2+hb}\right)$	(8c)
Thick-Walled Ellipsoid	Mirsky	$\sigma = \frac{Pb}{h}\left(1 - \frac{b^2}{2a^2} - \frac{h}{2b} - \frac{h^2}{8a^2}\right)$	(8d)

P, (LV pressure); a, (long axis radius); b, (short axis radius); h, (wall thickness); P is multiplied by 1.36 to convert mm Hg to g/cm^2.

Effects of Alterations of Aortic Pressure on LV Dimensions and Function

Hemodynamics

After filming the LV angiograms at twelve months of age, the following protocol was completed on ten of eleven dogs. The purpose of this study was to evaluate the effects of alterations of aortic pressure on echocardiographic parameters of LV dimensions and function. A multisensor pressure catheter (72,73) was inserted via the right carotid artery of the anesthetized (Sodium pentobarbital, 25mg/Kg) foxhounds lying in a left lateral position until LV and aortic pressure signals were obtained and recorded. Simultaneous and continuous M-mode echocardiograph recordings were obtained of the LV minor axis, using techniques as previously described (M-mode echo techniques). A control period was determined by stable LV and aortic pressure tracings and an echocardiogram demonstrating clear endocardial border resolution. After hemodynamic and echocardiographic tracings of the control period were recorded, intravenous infusions of phenylephrine and nitroprusside were administered in random fashion. Phenylephrine was infused at a dose (20-65 μg/min) sufficient to raise LV systolic pressure approximately 30 mm Hg and nitroprusside was given in a dose (100-250 μg/min) sufficient to decrease LV systolic pressure approximately 30 mm Hg. Between each infusion period and at the end of this experimental protocol, the hemodynamic and echocardiographic parameters were allowed to return to control levels (Figure 10).

The echocardiographic recordings were digitized and data were obtained by computer analysis by methods previously described (M-mode echo techniques). In addition to data obtained from the pressure

Figure 10. (Top) M-mode echocardiograms, LV and aortic pressure tracings obtained during the CON (Control), PE (phenylephrine) and NP (nitroprusside) periods. (Bottom) Computer tracings of D DIM/DT/DIM (normalized rate of dimension change) obtained by digitizing the septal and posterior wall endocardial borders from the M-mode echocardiograms in the upper panels.

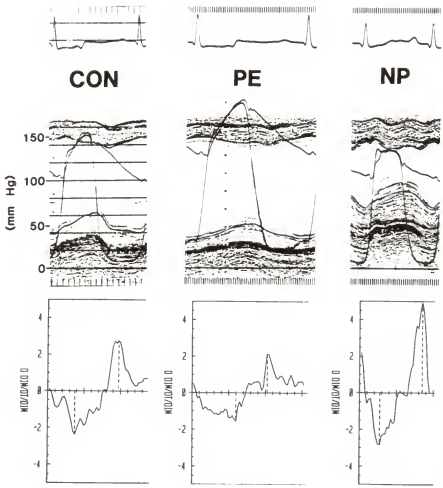
CON
PE
NP
(mm Hg)
150
100
50
0
4
2
0
-2
-4

recordings, left ventricular circumferential wall stress was determined at the different loading conditions. Wall stress was determined at peak -dD/dt/D using the echocardiographic dimension, wall thickness and LV pressure recorded at that point in the cardiac cycle. Circumferential wall stress was calculated using the simple thin-walled spherical Laplace model (8a).

Quantitation of Aortic Insufficiency

During the control period of the ventricular loading study, the phasic velocity of aortic blood flow was measured using the same multisensor pressure catheter which also contained an electromagnetic velocity transducer mounted 7 cm from the tip (78,79). The velocity transducer was calibrated in an in vitro steady flow hydraulic model using isotonic saline as previously described by our laboratory (79). The model consisted of a reservior attached to a length of Tygon tubing which had an internal diameter of 9 mm. The velocity transducer was determined by varying the flow rate from 10 to 100 cm/sec. The electrical output of the Biotronix flowmeter (BL-613) was linear over the range of flow velocities tested. The calibration factor for this velocity transducer was 24.5 cm/sec.

The multisensor catheter was introduced through the right carotid artery and the velocity transducer positioned in the ascending aorta. Internal cross-sectional area of the ascending aorta was calculated from measurement of the aortic root diameter made from the aortic root angiogram at end diastole. Measurement of aortic root diameter was assumed to be at the same approximate level as the velocity transducer.

Aortic root blood flow was calculated as the product of the area under the pulsatile velocity tracing and the aortic cross-sectional area. After pulsatile velocity recordings were made, the velocity transducer was withdrawn into the carotid artery where a transient occlusion of carotid artery blood flow was obtained. This was needed to establish an *in vivo* hydraulic zero (zero flow) for calibration of the velocity transducer (79). The product of this area and the aortic cross-sectional area, determined from aortic root angiography, represents the total forward stroke volume. Similarly, regurgitant stroke volume was calculated using the planimetered area below the zero flowline (Figure 11). The ratio of the regurgitant stroke volume to the total forward stroke volume multiplied by 100 represents the regurgitant fraction (RF). The regurgitant fraction averaged over 2-3 consecutive beats for each AI dog was then compared to the semi-quantitative estimate of the severity of AI as described in the section on aortic angiography.

Variability of Serial Echocardiographic Measurments

A study on five foxhounds was done to evaluate reproducibility of serial echocardiographic measurements. From this, the variability of each echocardiographic parameters was assessed. Five M-mode echocardiograms were obtained on five of the dogs as previously described over a twenty-one day period. Three to five consecutive cardiac cycles from these echoes were digitized. Variability of serial echocardiographic measurements of end diastolic and end systolic dimensions, posterior

Figure 11. Pulsatile tracings of aortic root blood velocity taken from three animals. The curve above the dashed line represents forward flow and the darkened curve below the dashed line represents regurgitant flow.

AORTIC ROOT BLOOD VELOCITY

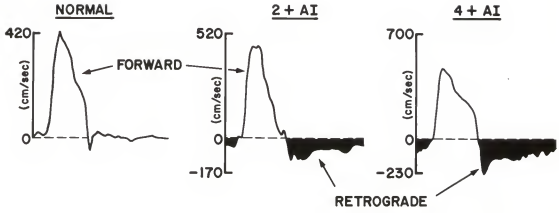

wall thickness, shortening fraction, and the peak rates of left ventricular emptying and filling (peak - and +dD/dt/D) were evaluated.

Statistical Analysis

Serial echocardiographic data were analyzed using a repeated measures analysis of variance which compared average response of both control and AI groups for each variable and then analyzed possible trends for each group as a function of time (80). This analysis was done to answer the following questions: 1) is there a significant difference between the average response of the two groups with the time factor collapsed; 2) are there any significant time differences independent of the group (i.e. with the groups collapsed); and 3) are there any significant differences in time within each group? Data which revealed a significant difference in time within each group were further examined using a two way analysis of variance and the Duncan's multiple range test for variable responses. These analyses revealed the group in which these time differences occurred and at what point in time these differences became significant. An analysis of covariance was performed to compare the slope of these trends for each variable on the control and AI group from both four to sixteen months of age and from six to sixteen months of age. Both angiographic and wall stress data were evaluated using a two way analysis of variance which analyzed the average response of the AI group as a function of time. Comparisons between the control and AI group data at the corresponding point in time were done using the student's unpaired t test. The

ventricular-loading study and the 2D echo data were analyzed using the appropriate student's t tests for multiple comparisons. Variability of serial echocardiographic measurements was evaluated using an analysis of variance to estimate the reliability of measurements (80). The coefficient of variation (standard deviation/mean) was used as an estimate of the variance. All data were expressed as the mean ± standard error of the mean and for all tests done, and $p<.05$ was considered statistically significant unless otherwise stated.

RESULTS

Angiographic Estimate of the Severity of Aortic Insufficiency

At the time AI was created, the severity of the insufficiency determined angiographically was 2+ in five dogs, 3+ in one and 4+ in one dog. There was no evidence for important change in angiographic severity of AI at either seven or twelve months of age in any of these dogs. Also, aortic root angiography of the control group at twelve months of age demonstrated competent aortic valves in all four animals.

Serial M-Mode Echocardiography

Table 3 summarizes serially obtained echocardiographic data. These echocardiographic findings which document the alterations in left ventricular dimensions, wall thickness and parameters of systolic function after the creation of AI are examined in detail in the following section.

Body Weight

Total body weight was 10.0 $\pm$ 0.2 kg and 10.2 $\pm$ 0.6 kg in the control and AI groups respectively, at four months of age. There was

TABLE 3
SERIAL ECHOCARDIOGRAPHIC DATA

Parameter	Group	Age (months) 4(before AI)	4.25	5	6	7	10	13	16
TOTAL BODY WEIGHT(kg)	CON	10.0 ± 0.2	-	13.5 ± 0.2	16.3 ± 0.3	18.6 ± 0.4	22.6 ± 0.9	24.9 ± 1.3	26.6 ± 1.4
	AI	10.2 ± 0.6	-	13.1 ± 0.5	15.5 ± 0.5	17.9 ± 0.7	22.4 ± 0.5	24.6 ± 0.5	26.8 ± 0.4
HEART RATE (bpm)	CON	134 ± 17	-	-	133 ± 5	131 ± 10	142 ± 7	140 ± 5	137 ± 4
	AI	130 ± 11	132 ± 7	122 ± 4	121 ± 7	111 ± 5	118 ± 8	124 ± 4	123 ± 6
END DIASTOLIC DIMENSION(mm)	CON	32.4 ± 0.9	-	-	36.3 ± 1.1	35.3 ± 0.9	37.4 ± 1.4	40.1 ± 1.6	40.4 ± 2.4
	AI	33.2 ± 1.1	37.9 ± 0.9	40.4 ± 1.5	41.8 ± 2.3	43.9 ± 2.4	46.2 ± 2.5	46.0 ± 2.4	49.5 ± 2.2
END SYSTOLIC DIMENSION(mm)	CON	20.8 ± 1.5	-	-	24.4 ± 0.9	23.7 ± 0.6	24.6 ± 0.8	26.9 ± 0.9	29.0 ± 1.9
	AI	20.4 ± 1.2	24.1 ± 1.6	26.8 ± 1.4	29.5 ± 2.3	29.9 ± 2.6	31.2 ± 2.8	32.9 ± 2.0	38.2 ± 2.1
POSTERIOR WALL THICKNESS(mm)	CON	6.22 ± .50	-	-	6.54 ± .27	7.20 ± .52	7.79 ± .31	7.88 ± .20	8.08 ± .23
	AI	6.14 ± .29	6.06 ± .57	6.72 ± .32	6.42 ± .33	7.67 ± .15	9.16 ± .45	9.54 ± .30	8.98 ± .59
SEPTAL WALL THICKNESS(mm)	CON	7.55 ± .32	-	-	7.00 ± .62	8.27 ± .33	8.15 ± .32	8.84 ± .40	8.62 ± .19
	AI	6.84 ± .53	7.21 ± .40	6.92 ± .42	7.45 ± .18	7.11 ± .27	8.13 ± .29	8.89 ± .53	8.95 ± .23
R/h RATIO	CON	2.69 ± .24	-	-	2.74 ± .24	2.49 ± .25	2.41 ± .16	2.59 ± .16	2.53 ± .20
	AI	2.78 ± .18	3.26 ± .28	3.06 ± .15	3.29 ± 1.6	2.87 ± .16	2.44 ± .20	2.44 ± .13	2.83 ± .26
SHORTENING FRACTION(%)	CON	36.0 ± 2.9	-	-	32.5 ± 1.6	32.0 ± 2.0	33.1 ± 1.5	32.7 ± 2.4	30.3 ± 1.3
	AI	38.6 ± 2.6	35.5 ± 3.0	33.8 ± 1.8	30.1 ± 2.0	32.0 ± 2.6	31.7 ± 2.5	28.6 ± 1.2	22.3 ± 1.3
PEAK -dD/dt/D (sec^{-1})	CON	4.18 ± .55	-	-	3.77 ± .34	3.77 ± .22	4.22 ± 2.7	3.97 ± .36	3.54 ± .29
	AI	4.71 ± .51	4.55 ± .70	3.59 ± .30	3.39 ± .31	3.52 ± .38	3.52 ± .35	3.10 ± .15	2.41 ± .19
PEAK +dD/dt/D (sec^{-1})	CON	5.72 ± .75	-	-	4.97 ± .30	5.25 ± .50	4.94 ± .35	4.90 ± .23	4.00 ± .77
	AI	6.32 ± .69	5.55 ± .63	4.56 ± .40	3.92 ± .41	4.06 ± .48	3.85 ± .53	3.31 ± .40	2.73 ± .22

Mean ± S.E.M.; CON(N=4), AI(N=7)

was no significant difference in the rate of growth between the two groups during the entire study as illustrated in Figure 12. Total body weight at sixteen months of age averaged 26.5 ± 0.4 kg in the AI group. Therefore, data presented in this study were not normalized for total body weight because of the similar growth rate and the minimal variability in weight between all eleven animals (between subject variability).

Heart Rate

The mean heart rate was 134 ± 17 bpm in the Control group and 130 ± 11 bpm in the AI group at four months of age (before AI). There were no significant differences in heart rate between the two groups during the entire study (Figure 13). There did not appear to be an obvious influence of acclimatization or maturity of the animals on the heart rate as the study progressed.

Left Ventricular Internal Dimensions

At four months of age (before AI), EDD was 32.4 ± 0.9 mm and 33.2 ± 1.1 mm in the Control and AI groups respectively, and was not significantly different. Comparison of end diastolic dimension (EDD) after AI was created revealed significant differences between the two groups ($p < .0001$; Figure 14). The initial rate of EDD increase was significantly greater in the AI group through six months of age. This increase was detectable at one week after AI and continued to increase throughout the study as EDD at fifteen and sixteen months of age was significantly greater than at nine months. However, there was no

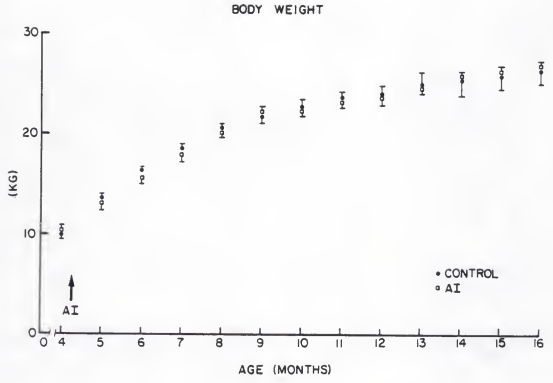

Figure 12. There was no significant difference in total body weight between the two groups during the in year study period. Data are expressed as Mean ± S.E.M.

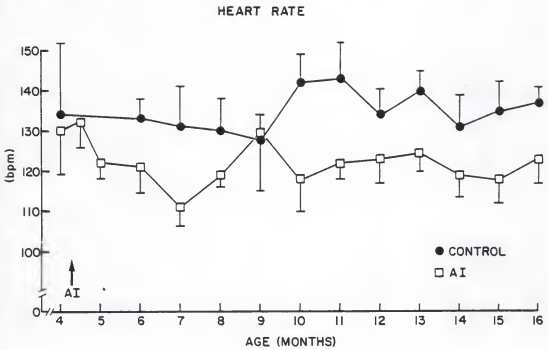

Figure 13. Heart rate obtained from standard limb lead electrocardiograms. There was no significant difference between the two groups. Data are expressed as Mean ± S.E.M.

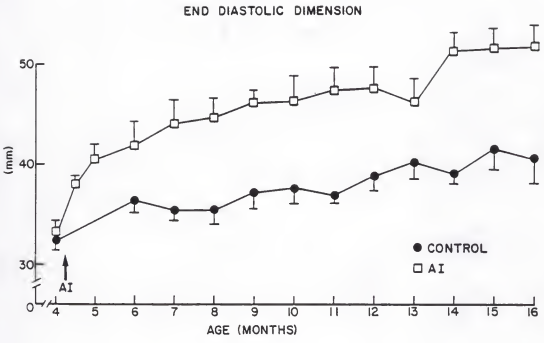

Figure 14. End diastolic dimension (EDD) was significantly increased in the AI group when compared to the Control group ($p < .0001$). EDD increase was detected one week after AI. However, there was no significant difference on the rate of EDD increase from six to sixteen months of age between the two groups. Data are expressed as Mean ± S.E.M.

significant difference in the rate of EDD increase from six (2 months after AI) to sixteen months of age between the two groups. Analysis of alterations in end systolic dimension (ESD) demonstrated differences between the two groups ($p < .0001$) after AI were similar to those observed with the EDD (Figure 15). There was no difference in the ESD at four months of age (before AI) between Control and AI group (20.8 ± 1.5 mm vs. 20.4 ± 1.2 mm, respectively). After creation of AI, the rate of ESD increase was greater through six months of age as compared to the Control group. This difference was significant at one week after AI and continued to increase throughout the study period. ESD in the AI group from fourteen to sixteen months of age was significantly greater than at nine months. Nevertheless, there was no significant difference in the rate of ESD increase from six (2 months after AI) to sixteen months of age between the two groups. Figure 5 illustrates the echocardiographic changes observed in a Control and AI dog at four, six, ten and sixteen months of age. It should be apparent that the major changes in left ventricular internal dimensions occurred between four and six months of age.

Wall Thickness

Left ventricular posterior wall thickness (PWT) averaged 6.22 ± 0.5 mm in the Control group and 6.14 ± 0.3 mm in the AI group at four months of age (before AI). This difference was not significant. However, there was a significantly ($p < .04$) greater rate of increase in PWT in the AI group throughout the study when compared to the Control group (Figure 16). Trend analysis of the AI group alone revealed this

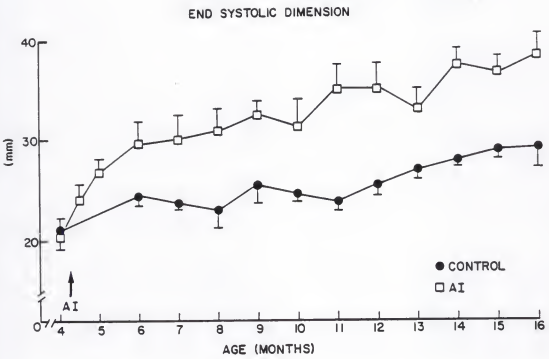

Figure 15. End systolic dimension was significantly increased in the AI group when compared to the Control group ($p < .0001$). ESD increase was detected one week after AI. However, there was no significant difference in the rate of ESD increase from six to sixteen months of age between the two groups. Data are expressed as Mean ± S.E.M.

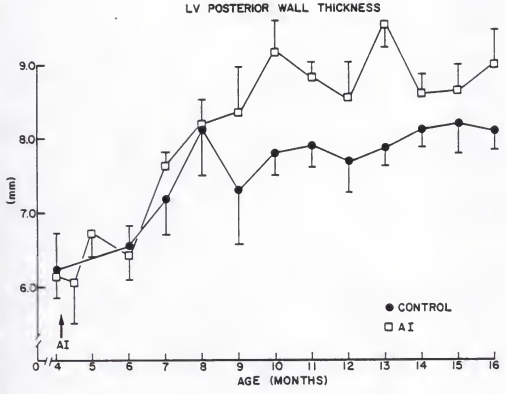

Figure 16. Rate of increase of left ventricular posterior wall thichness was significantly greater in the AI group when compared to the Control group ($p < .04$). This increase in posterior wall thickness was detected at seven months of age. The overall rate of posterior wall thickening was 0.24 mm/month. Data are expressed as Mean ± S.E.M.

increase in PWT was evident by seven months of age (7.67 ± .15 mm) and increased significantly to 8.98 ± .50 mm at sixteen months. A similar pattern of left ventricular wall growth was observed in the changes in septal wall thickness (SWT). Mean SWT was 7.55 ± .32 mm in the Control group and 6.84 ± .53 mm in the AI group at four months of age (before AI) and was not significantly different. The rate of SWT increase appeared to be greater ($p<.07$) in the AI group when compared to the Controls throughout the one year study period (Figure 17). This increase was detected in the AI group by eight months of age (8.52 ± .23 mm) and continued to increase through sixteen months (8.95 ± .23 mm).

R/h Ratio

The ratio of the ventricular minor axis radius to the PWT at end diastole, known as the R/h ratio, did not reveal a significant trend in the Control group. It averaged 2.69 ± .24 at four months of age (before AI) and remained within a range of 2.1-2.8 throughout the study. In the AI group, the R/h ratio was 2.78 ± .18 one week after AI, and remained above the pre-AI level until four months after AI (Figure 18). Beginning at five months after AI (nine months of age), there was no significant difference in the R/h ratio between the two groups as the AI group developed a thicker posterior wall which normalized the R/h ratio.

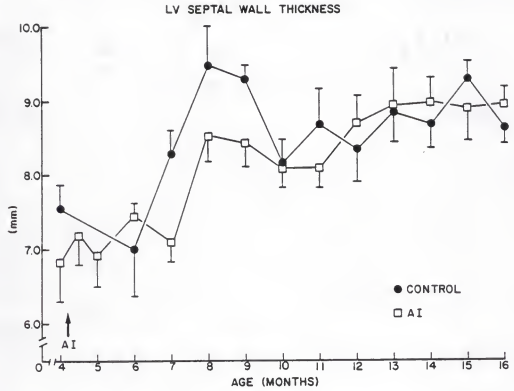

Figure 17. Rate of increase of left ventricular septal wall thickness was not significantly different between the two groups ($p < .07$). The overall rate of septal wall thickening in the AI group was 0.18 mm/month. Data are expressed an Mean ± S.E.M.

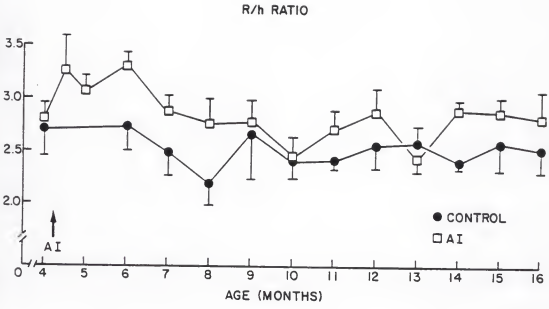

Figure 18. The R/h ratio (rate of left ventricular minor axis radius to posterior wall thickness at end diastole) in the AI group was singificantly increased from one week after AI through four months after AI (eight months of age) when compared to the pre-AI level ($p < .05$). Data are expressed as Mean ± S.E.M.

Shortening Fraction

Comparison of shortening fraction (SF), a parameter of systolic function, did not reveal an overall significant difference ($p<.08$) between the two groups. SF was not significantly different at four months of age, before AI ($36.0 \pm 2.9\%$ and $38.6 \pm 2.6\%$ in the Control and AI groups, respectively). However, a significant decrease in the AI group to $33.8 \pm 1.8\%$ ($p< .05$) was detected one month after AI (Figure 19). Although somewhat variable, SF continued to decrease in the AI group throughout the study period. SF from fourteen to sixteen months of age in the AI group was significantly less than at ten months of age. In contrast, SF in the Control group remained unchanged throughout the study.

Peak Rate of Dimension Change

Peak normalized rate of left ventricular emptying or shortening is represented by peak -dD/dt/D. Comparison of the two groups demonstrated a significant difference ($p<.01$) in peak -dD/dt/D (Figure 20). At four months of age (before AI), the peak -dD/dt/D was $4.18 \pm .55$ sec^{-1} in the Control group and $4.71 \pm .51$ sec^{-1} in the AI group and was not significantly different. A decrease in peak -dD/dt/D to $3.59 \pm .30$ sec^{-1} in the AI group was detected at five months of age (one month after AI). This parameter continued to decrease to $2.41 \pm .19$ sec^{-1} at sixteen months of age which was significantly less than at ten months. Furthermore, and similar to the pattern observed in SF, there was no significant change in peak -dD/dt/D throughout the study in the Control group.

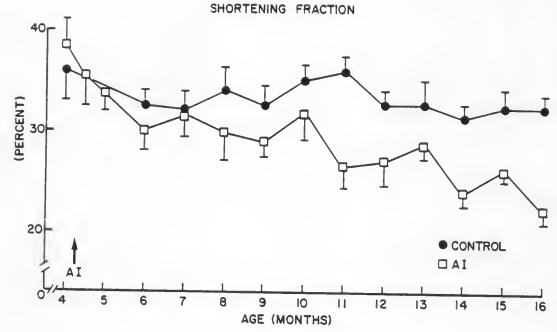

Figure 19. A significant decrease in shortening fraction in the AI group was detected one month after AI ($p < .05$). The rate of shortening fraction decrease in the AI group was 0.77%/month. Data are expressed and Mean ± S.E.M.

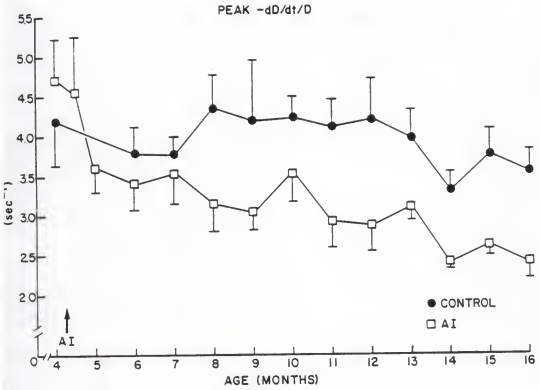

Figure 20. Peak -dD/dt/D was significantly decreased in the AI group when compared to Controls ($p < .01$). This decrease was detected one month after AI and the overall rate of decrease in the AI group was 0.11 sec^{-1}/month. Data are expressed as Mean ± S.E.M.

Peak normalized rate of left ventricular filling, represented by peak +dD/dt/D is a parameter describing diastolic characteristics of the left ventricle. Analysis of this parameter yielded a pattern of change similar to that of peak -dD/dt/D. There was no significant difference between the two groups at four months of age, before AI ($5.72 \pm .75$ sec^{-1} and $6.32 \pm .69$ sec^{-1} in the Control and AI groups, respectively). A significant decrease in peak +dD/dt/D was first demonstrated at five months of age ($4.56 \pm .40$ sec^{-1}) and continued to decrease to $2.73 \pm .22$ sec^{-1} at sixteen months of age (Figure 21). Once again the Control group did not demonstrate any significant changes throughout the one year study period.

Serial Echocardiographic Variability

An analysis of variance to evaluate the variability of serial echocardiographic data did not reveal any significant differences in measurements of EDD, ESD, PWT, SF, peak -dD/dt/D and peak +dD/dt/D obtained on different days (Table 4). The coefficient of variation for these parameters were as follows: EDD - 1.8%, ESD - 4.3%, PWT - 7.6%, SF - 7.8%, peak -dD/dt/D - 19.8%, and peak +dD/dt/D - 23.2%.

Serial LV Angiography

Alterations in left ventricular end diastolic volume (EDV) and end systolic volume (ESV) were similar in all equations used to calculate the volume (Table 5). Using the corrected Dodge equation, EDV in the

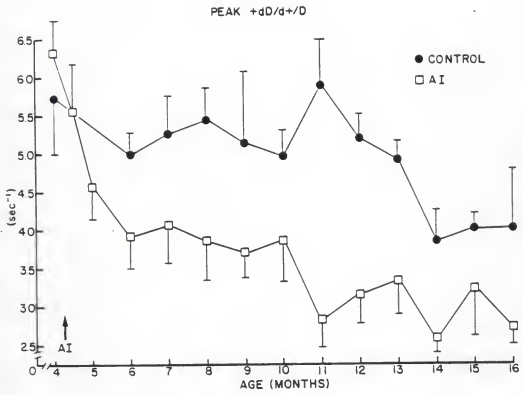

Figure 21. Peak +dD/dt/D was significantly decreased in the AI group when compared to the Controls ($p < .01$). This decrease was detected one month after AI. Data are expressed as Mean ± S.E.M

TABLE 4
REPRODUCIBILITY OF SERIAL ECHOCRADIOGRAPHIC MEASUREMENTS

Parameter	Day 1	Day 2	Day 3	Day 4	Day 5	Mean	S.D.	Coefficient of Variation	95% Probability of true change
EDD (mm)	44.2	43.8	43.4	43.4	43.8	43.7	0.80	1.8	1.6
ESD (mm)	28.6	29.0	28.4	28.4	28.0	28.3	1.23	4.3	2.5
SF (%)	34.0	33.2	34.0	34.0	35.5	34.6	2.71	7.8	5.4
PWT (mm)	9.0	8.4	8.4	8.4	8.0	8.4	0.64	7.6	1.3
peak -dD/dt/D (sec^{-1})	3.6	3.7	4.0	4.0	4.2	3.9	0.76	19.8	1.5
peak +dD/dt/D (sec^{-1})	4.9	3.8	4.6	4.6	4.7	4.6	1.07	23.2	2.1

Data for each day represents the mean for all 5 animals. EDD (End diastolic dimension); ESD (End systolic dimensions); SF (Shortening fraction); PWT (Posterior wall thickness); peak -dD/dt/D (peak rate of left ventricular emptying); peak +dD/dt/D (peak rate of left ventricular filling).

TABLE 5
SERIAL ANGIOGRAPHIC QUANTITATION OF LV VOLUME AND EJECTION FRACTION

	Equation		Age (months) 4 EDV (ml)	4 ESV (ml)	4 EF (%)	7 EDV (ml)	7 ESV (ml)	7 EF (%)	12 EDV (ml)	12 ESV (ml)	12 EF (%)
CONTROL (N=4)	Dodge	(4)							71 ± 4.7	26 ± 3.5	64 ± 4.5
	Corrected Dodge	(6a)							62 ± 4.3	21 ± 3.2	66 ± 4.6
	Greene	(5)							82 ± 2.9	29 ± 4.5	65 ± 6.6
	Corrected Greene	(6b)							67 ± 2.3	25 ± 3.5	62 ± 6.4
AI (N=6)	Dodge	(4)	45 ± 6.2	17 ± 2.3	61 ± 2.9	105 ± 7.1[a]	38 ± 2.8[b]	64 ± 3.1	128 ± 11.0[a]	59 ± 5.0[c]	54 ± 1.1[d]
	Corrected Dodge	(6a)	39 ± 5.6	14 ± 2.1	65 ± 3.0	93 ± 6.4[a]	32 ± 2.6[b]	65 ± 3.1	115 ± 10.0[a]	52 ± 4.5[c]	55 ± 1.1[d]
	Greene	(5)	45 ± 4.8	18 ± 2.9	62 ± 2.7	120 ± 11.1[a]	37 ± 3.1[b]	68 ± 3.9	149 ± 12.3[a]	67 ± 6.7[c]	55 ± 3.3[d]
	Corrected Greene	(6b)	38 ± 3.8	16 ± 2.2	57 ± 2.4	96 ± 8.7[a]	32 ± 2.4[b]	66 ± 3.8	119 ± 9.6[a]	55 ± 5.3[c]	54 ± 3.3[d]

Mean ± S.E.M.; EDV (End Diastolic Volume; ESV (End Systolic Volume); EF (Ejection Fraction)
a: $p < .05$ vs. 4 mos.; b: $p < .05$ vs. 4, 12 mos.; c: $p < .05$ vs. 4, 8 mos.; d: $p < .05$ vs. Control

AI group was 39.4 ± 5.6 ml at four months of age (before AI) and increased significantly ($p<.05$) to 93.4 ± 6.4 ml at seven months (Figures 22,23). EDV continued to increase, although not significantly, to 114.8 ± 10.0 ml at twelve months of age (eight months after AI). Rate of EDV increase was remarkably similar to the rate of EDD increase in the AI group as shown in Figure 24. In comparison, EDV in the Control group at twelve months was 65.6 ± 4.6 ml. Similarly, ESV in the AI group increased significantly ($p<.05$) from 13.8 ± 2.1 ml at four months of age to 32.2 ± 2.6 ml at seven months. Furthermore, ESV continued to show a significant increase ($p<.05$) to 51.6 ± 4.5 at twelve months of age (eight months after AI). Once again, comparison to the ESV of the Control group at twelve months (21.4 ± 3.2 ml) demonstrated the magnitude of the volume overload in the AI group.

Ejection fraction (EF) did not change from four (before AI) to seven months of age in the AI group. Using the corrected Dodge formula, EF was 64.7 ± 3.0% at four months and 64.9 ± 3.1% at seven months. At twelve months of age, there appeared to be a decrease in EF to 55.0 ± 1.1% (Figure 25). However, statistical significance of this decrease was dependent upon the equation used to calculate LV volume (Table 5). The decrease in EF was significant ($p<.05$) when the Greene and corrected Greene equations were used, but only of borderline significance ($p<0.1$) when the corrected Dodge equation was used. In contrast, comparison of EF in the AI group to the Control group at twelve months of age revealed a statistically significant difference ($p<.05$) only when the Dodge and corrected Dodge equations were used (Table 5). Rate of decline in EF in the AI group was also less than

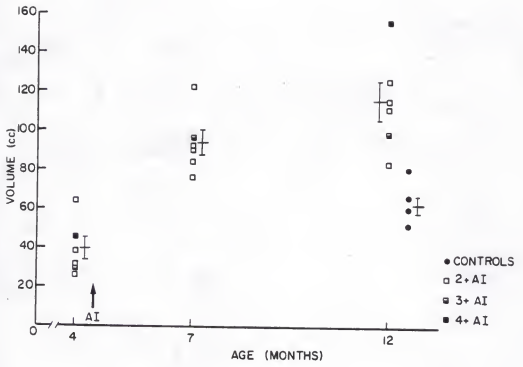

Figure 22. Angiographic end diastolic volume (EDV) using the corrected Dodge equation ($Vc = 0.91V_D - 1.97$) at four (before AI), seven and twelve months of age. EDV was significantly increased at seven months of age when compared to the pre-AI level ($p < .05$). Data are expressed as both individual data points and as a Mean ± S.E.M.

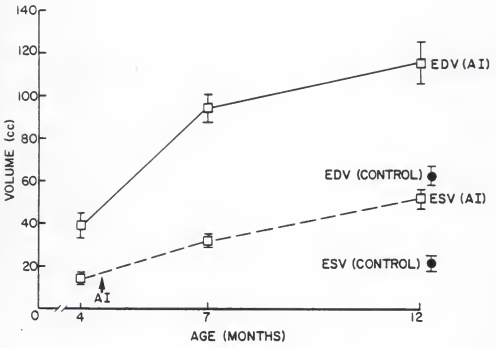

Figure 23. Angiographic end diastolic (EDV) and end systolic (ESV) volume using the corrected Dodge equation ($Vc=0.91V_D-1.97$) at four (before AI), seven and twelve months of age. Both EDV and ESV were significantly increased at seven of age when compared to the pre-AI level ($p< .05$). ESV was also significantly increased at twelve months of age when compared to seven months ($p< .05$). Data are expressed as Mean ± S.E.M.

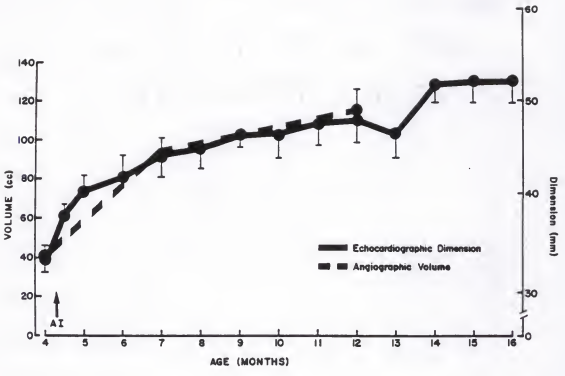

Figure 24. Comparison of serial changes in end diastolic angiographic volume (EDV) and echocardiographic dimension (EDD) in the AI group. Data are expressed as Mean ± S.E.M.

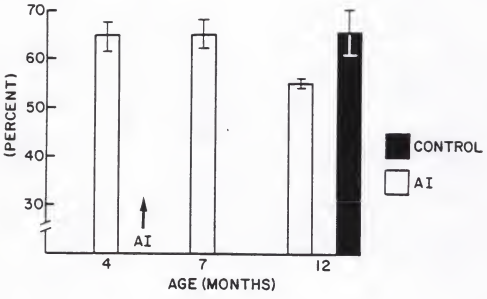

Figure 25. Angiographic ejection fraction using the corrected Dodge equation ($Vc=0.91V_D-1.97$) at four (before AI), seven and twelve months of age. Ejection fraction in the AI group was significantly decreased at twelve months of age when compared to the Controls ($p< .05$). Data are expressed as Mean ± S.E.M.

the rate of decline observed in echocardiographically derived shortening fraction (Figure 26).

Serial LV Circumferintial Wall Stress

Analysis of LV circumferential end diastolic (EDWS) and end systolic wall stress (ESWS) revealed some important trends. However, scatter in the data may have been due to variability in the angiographic measurement of long and short axes and wall thickness during both end diastole and end systole. Because of the variability and the small number of animals involved, these trends were tested for significance at the $p<0.1$ level (Table 6).

Using the data calculated from Mirsky's equation for wall stress as an example, EDWS increased significantly in the AI group from 16.6 ± 3.2 g/cm^2 at four months of age (before AI) to 38.6 ± 2.7 g/cm^2 at seven months (Figure 27). Although EDWS decreased to 26.4 ± 7.0 g/cm^2 ($p<0.1$) at twelve months, this value was still significantly above the level of EDWS before AI ($p<0.1$). Also, there was no difference in EDWS when the AI group at four months of age (before AI) was compared to the Control group at twelve months (16.6 ± 3.2 g/cm^2 vs. 16.9 ± 2.8 g/cm^2). Similarly, ESWS increased significantly ($p<0.1$) in the AI group from 112.5 ± 14.4 g/cm^2 at four months of age (before AI) to 180.8 ± 28.2 g/cm^2 at seven months (Figure 27). ESWS decreased by twelve months to 133.6 ± 20.8 which was not different from its pre-AI level. Once again, comparison of the Control group ESWS at

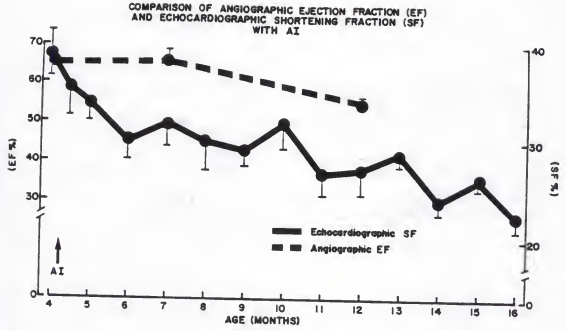

Figure 26. Comparison of serial changes of angiographic ejection fraction (EF) and echocardiographic shortening fraction (SF) in the AI group. SF is significantly decreased one month after AI and EF is decreased eight months after AI. Data are expressed as Mean ± S.E.M.

TABLE 6
SERIAL LV CIRCUMFERENTIAL WALL STRESS

	EQUATION	4 EDWS (g/cm^2)	4 ESWS (g/cm^2)	7 EDWS (g/cm^2)	7 ESWS (g/cm^2)	12 EDWS (g/cm^2)	12 ESWS (g/cm^2)
CONTROL (n=4)	La Place (7a)					14 ± 2.1	76 ± 6.8
	Sandler and Dodge (7b)					23 ± 3.7	144 ± 12.0
	Falsetti (7c)					21 ± 3.3	111 ± 11.6
	Mirsky (7d)					17 ± 2.8	72 ± 13.0
AI (n=6)	La Place (7a)	12 ± 2.2	111 ± 10.6	28 ± 1.9	152 ± 19.8	22 ± 4.7	132 ± 16.5
	Sandler and Dodge (7b)	21 ± 3.6	203 ± 16.2	47 ± 2.9	275 ± 32.5	37 ± 7.9	227 ± 25.8
	Falsetti (7c)	19 ± 3.5	180 ± 13.6	44 ± 2.7	251 ± 28.8	31 ± 7.5	193 ± 22.5
	Mirsky (7d)	17 ± 3.2	113 ± 14.4	39 ± 2.7	181 ± 28.2	26 ± 7.0	134 ± 20.8

MEAN ± S.E.M.; EDWS (End Diastolic Wall Stress); ESWS (End Systolic Wall Stress)
a: $p < 0.1$ vs 4, 12 mos.; b; $p < 0.1$ vs 4 mos.

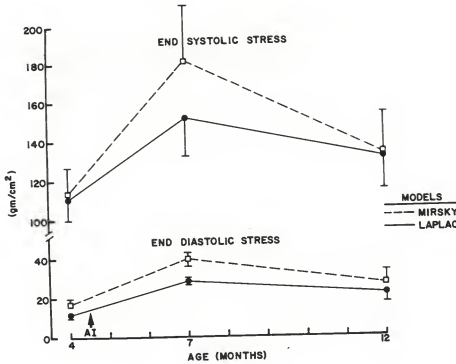

Figure 27. Serial changes in LV circumferential wall stress in the AI group at four (before AI), seven and twelve months of age. (Top) End systolic wall stress was increased at seven months of age ($p < 0.1$) and returned to the pre-AI level at twelve months. (Bottom) End diastolic wall stress was increased at seven months of age ($p < 0.1$) and remained elevated at twelve months. Data are expressed as Mean ± S.E.M.

twelve months of age (71.8 ± 13.0 g/cm^2) to the AI group at four months of age did not reveal a significant difference.

Effects of Alterations of Aortic Pressure on LV Dimensions and Function

Quantitation of Aortic Insufficiency Using a Catheter-tip Velocity Velocity Transducer

Aortic root blood velocity tracings were analyzed to provide information concering total, forward and regurgitant stroke volume and regurgitant fraction (RF). These data are summarized in Table 7. Total stroke volume averaged 46 ± 6.2 ml in the Control group and 80 ± 14.5 ml in the AI group. Mean forward and regurgitant stroke volume in the AI group were 46 and 34 mls, respectively, and regurgitant fraction was 43 ± 8.9%. Although these data are also categorized by their angiographic severity of AI, the small numbers in each subgroup prevented any statistical correlation between angiographic severity and regurgitant fraction.

Hemodynamics

During this ventricular loading study at twelve months of age (eight months after AI), Control dogs were alternatively called the Normal (NOR) group in order to avoid confusion with the designated hemodynamic intervals. There were no significant differences in pressure between Normal and AI groups during any of these three periods: control, phenylephrine or nitroprusside (Figure 28). During the control period, aortic pressure in the Normals was 118/84 mm Hg

TABLE 7
QUANTITATION OF AORTIC INSUFFICIENCY

	Total Stroke Volume (ml)	Forward Stroke Volume (ml)	Regurgitant Stroke Volume (ml)	Regurgitant Fraction (%)
Control (n=4)	46 ± 10.4	46 ± 10.4	-	-
AI				
2+ (n=3)	76 ± 26.2	54 ± 24.5	22 ± 5.1	33 ± 9.5
3+ (n=1)	83	42	41	49
4+ (n=1)	88	26	61	70
Mean (n=5)	80	46	34	43
S.E.M.	14.5	14.5	8.3	8.9

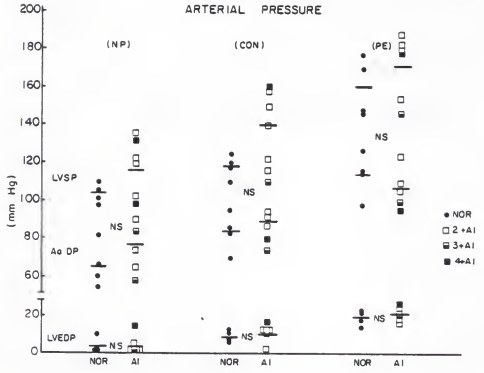

Figure 28. There was no significant difference in arterial pressure between the two groups during the NP (nitroprusside), Con (control) and PE (phenylephrine) periods. LVSP (left ventricular systolic pressure); Ao DP (aortic diastolic pressure); LVEDP (left ventricular end diastolic pressure). Date are expressed as individual data points with the dark line representing the Mean.

(LV systolic/aortic diastolic pressure) and LV end diastolic pressure (LVEDP) averaged 8 mm Hg. For the AI group, aortic pressure was 140/91 mm Hg and LVEDP was 10 mm Hg. With phenylephrine infusion, the LV systolic pressure increased to 160 and 171 mm Hg. in the Normal and AI groups, respectively. There was a similar increase in the LVEDP to 19 mm Hg. in the Normals and to 21 mm Hg. with AI. Although it appeared that the pulse pressure (LV systolic - aortic diastolic pressure) was greater in the AI group during phenylephrine (Figure 28), this difference was not significant. During nitroprusside infusion, the aortic pressure decreased to 104/66 and 116/77 in the Normal and AI groups, respectively. LVEDP declined to 3 mm Hg. in both groups during this period.

Heart Rate

Heart rate in these anesthetized dogs during the control period was 85 $\pm$ 6.4 bpm in the Normals and 77 $\pm$ 8.3 bpm in the AI group and was not significantly different. There was no significant change in heart rate during the phenylephrine period in either group as shown in Figure 29. However, with nitroprusside infusion, there was a significant increase in heart rate to 126 $\pm$ 25.0 and 124 $\pm$ 18.4 in the Normal and AI groups, respectively.

End Diastolic Dimension

Comparison of end diastolic dimension (EDD) demonstrated that the AI group was significantly larger ($p<.01$) than the Normals during both control and phenylephrine periods (Figure 30). End diastolic dimension

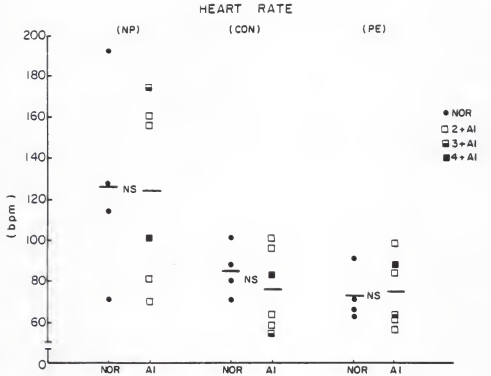

Figure 29. There was no significant difference in heart rate between the two groups during the NP (nitroprusside), Con (control) and PE (phenylephrine) periods. Heart rate was significantly increased in both groups during NP when compared to Con ($p < .05$). Data are expressed as individual data points with the dark line representing the Mean.

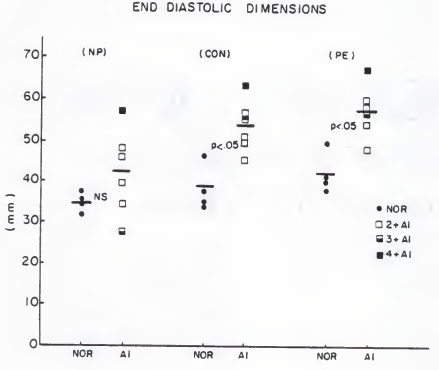

Figure 30. End diastolic dimension (EDD) was significantly increased in the AI group ($p < .05$) during both Con (control) and PE (phenylephrine) periods when compared to Nor (normals). In the AI group, EDD was significantly increased during PE when compared to the CON period ($p < .001$). Data are expressed as individual data points and the dark line represents the Mean.

was 38 ± 2.8 mm in the Normal and 53 ± 2.6 mm in the AI group during the control period. With phenylephrine, EDD in the AI group increased to 57 ± 2.5 mm (Figure 19, $p<.001$), whereas the Normal group did not increase. Also, during nitroprusside infusion, the AI group demonstrated a significant decrease ($p<.025$) in EDD to 42 ± 4.3 mm compared to 35 ± 1.0 mm in the Normal group which was not different from its control value.

Left Ventricular Systolic Function

Comparison of shortening fraction between the Normal and AI group did not reveal any significant differences during any of the three periods (Figure 31). However, the AI group demonstrated a significant decrease ($p<.001$) from 31 ± 1.8% during the control period to 23 ± 2.0% with phenylephrine. The Normal group did not show a decrease. However, the Normals did increase shortening fraction significantly from 32 ± 3.6% during the control period to 39 ± 3.6% with nitroprusside ($p< .05$).

Peak -dD/dt/D which represents the peak normalized rate of left ventricular shortening did not reveal a significant difference between groups during the control period. However, the AI group demonstrated a significant decrease ($p<.01$) from 2.34 ± .18 sec^{-1} during the control period to 1.61 ± .14 sec^{-1} with phenylephrine (Figures 10, 32). In contrast, the Normal group remained relatively unchanged from a control value of 2.80 ± .19 sec^{-1} to 2.55 ± .45 sec^{-1} with phenylephrine. This represented a 30% decrease in the peak rate of LV shortening in the AI group and only a 7% decrease in the Normal group.

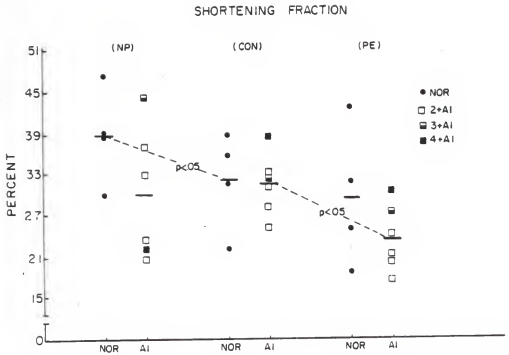

Figure 31. In the AI group, shortening fraction was significantly decreased ($p < .05$) during PE (phenylephrine) when compared to the CON (control) period. In the Nor (normal) group, shortening fraction demonstrated a significant increase ($p < .05$) during NP (nitroprusside) when compared to the CON period. Data are expressed as individual data points and the dark line represents the Mean.

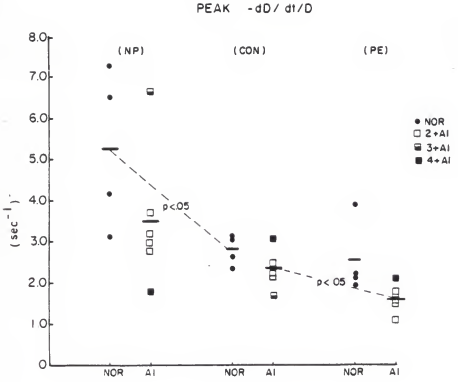

Figure 32. In the AI group, peak -dD/dt/D was significantly decreased ($p < .05$) during PE (phenylephrine) when compared to the CON (control) period. In the Nor (normal) group, peak -dD/dt/D demonstrated a significant increase ($p < .05$) during NP (nitroprusside) when compared to the CON period. Data are expressed as individual data points and the dark line represents the Mean.

With nitroprusside, only the Normal group demonstrated a significant increase ($p<.05$) in the peak rate of LV shortening when compared to the control period.

Although the aortic pressure was altered with phenylephrine and nitroprusside to a similar level in both Normal and AI groups, this may not accurately reflect the ventricular load at the time when peak rate of LV shortening was measured. Therefore, in order to examine alterations in LV systolic function more closely, peak rate of LV shortening was plotted against LV circumferential wall stress measured at peak shortening (Figure 33). Figure 34 is a closeup of the load-velocity curve demonstrating that peak rate of LV shortening was measured at similar levels of wall stress in the Normal and AI groups. LV wall stress measured at peak -dD/dt/D during the control period was 151 ± 11 g/cm^2 and 175 ± 13 g/cm^2 in the Normal and AI groups, respectively. Although there was approximately a 50% increase in the calculated wall stress in both groups during the phenylephrine period, the difference between the two groups was not significant (229 ± 27 g/cm^2 and 257 ± 22 g/cm^2, respectively). Therefore, a 30% decrease in peak rate of LV shortening observed in the AI group reflects a significant decrease in left ventricular function.

The end diastolic pressure-dimension relation, which characterizes some diastolic properties of the left ventricle (81-83) was diagrammed for all three periods in Figure 35. Although the AI curve is shifted to the right, there was no significant increase in slope (dP/dD) between control and phenylephrine periods when compared to the Normal group (Figure 36).

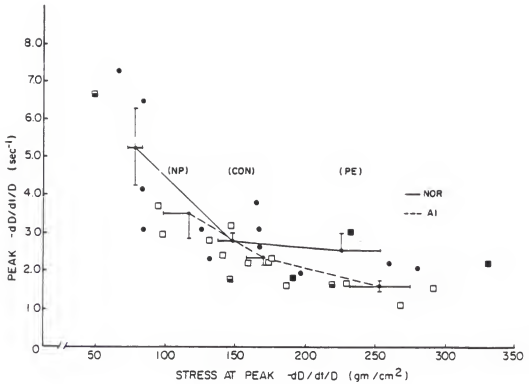

Figure 33. Relation between peak -dD/dt/D and LV circumferential wall stress during acute changes in ventricular load. NP (nitroprusside); CON (control); PE (phenylephrine). Data are expressed both as individual data points and as a Mean ± S.E.M.

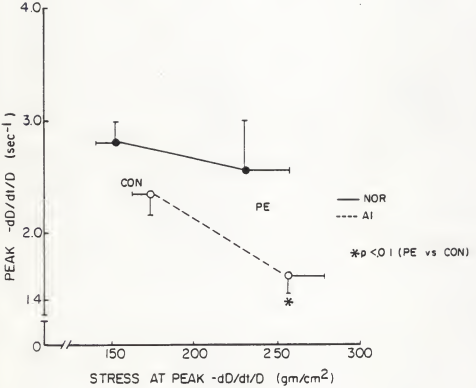

Figure 34. Closeup of Figure 33. Relation between peak -dD/dt/D and LV circumferential wall stress when ventricular load was altered with PE (phenylephrine). Peak -dD/dt/D in the AI group was significantly decreased ($p < .01$) during PE even though wall stress is similar to the Nor (normal) group. Data are expressed as Mean ± S.E.M.

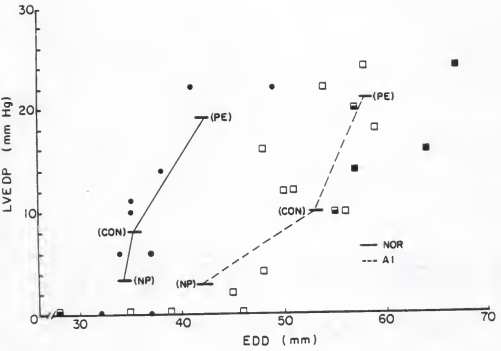

Figure 35. End diastolic pressure-dimension relation during acute changes in ventricular load. NP (nitroprusside); CON (control): PE (phenylephrine); LVEDP (left ventricular end diastolic pressure); EDD (end diastolic dimension). Data are expressed as individual data points and the dark line represents the Mean.

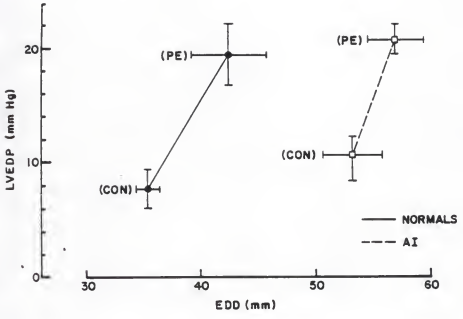

Figure 36. Closeup of Figure 35. End diastolic pressure-dimension relation when ventricular load was altered with PE (phenylephrine). Although the AI curve is shifted to the right, the slope (dP/dD) was not significantly different from the Normals. LVEDP (left ventricular end diastolic pressure); EDD (end diastolic dimension). Data are expressed as Mean ± S.E.M.

Two Dimensional Echocardiography

Left ventricular volume and mass were estimated using two dimensional (2D) echocardiographic techniques in ten of the eleven conscious dogs at twenty-four months of age (twenty months after AI; Table 8). Both left ventricular volume and mass were significantly larger in the AI group, while ejection fraction was significantly decreased when compared to the Control group. End diastolic volume averaged 60 $\pm$ 2.7 ml in the Control group and 98 $\pm$ 11.3 ml in the AI group ($p<.05$). The difference in end diastolic volume between Control and AI groups can be seen in the cross-sectional and long axis 2D echo views frozen in end diastole in Figure 37. End systolic volume was 24 $\pm$ 1.7 ml in the Control group and 49 $\pm$ 6.5 ml in the AI group ($p<.025$). Ejection fraction was 61 $\pm$ 1.4% in the Control group compared to 50.5 $\pm$ 1.3% in the AI group ($p<.001$). Left ventricular muscle mass at twenty-four months of age averaged 106 $\pm$ 1.3 gm in the Control group and 127 $\pm$ 7.1 gm in the AI group ($p<.05$).

TABLE 8
2D ECHO ESTIMATES OF LV VOLUME, MASS AND EJECTION FRACTION
AT 24 MONTHS OF AGE

	Dog No.	EDV (ml)	ESV (ml)	EF (%)	LV Mass (gm)	LV Mass (gm/kg body wt.)
CONTROL	53	63	26	59	105	3.89
	96	54	19	65	105	3.96
	98	56	23	59	109	4.04
	106	65	26	60	103	3.32
	MEAN	60	24	61	106	3.80
	S.E.M.	2.7	1.7	1.4	1.3	.16
AI	47	80	38	53	123	4.47
	52	102	55	46	138	4.93
	95	92	45	54	138	4.60
	97	86	41	52	101	3.81
	102	76	38	50	113	4.04
	105	151	79	48	147	5.55
	MEAN	98[a]	49[b]	51[c]	127[a]	4.57[a]
	S.E.M.	11.3	6.5	1.3	7.1	.26

Mean ± S.E.M.; EDV (End Diastolic Volume); ESV (End Systolic Volume); EF (Ejection Fration).
a: $p < .05$ vs. Control
b: $p < .025$ vs. Control
c: $p < .001$ vs. Control

Figure 37. Comparison of two-dimensional echocardiographic cross-sectional and long axis views "frozen" in end diastole for a Control and a 4+ AI dog at twenty-four months of age.

ONTROL

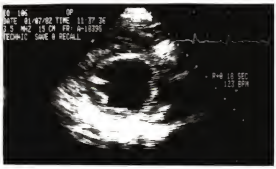

CROSS SECTION

LONG AXIS

4+ AI

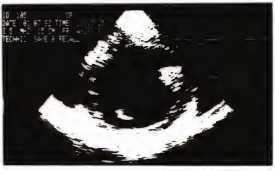

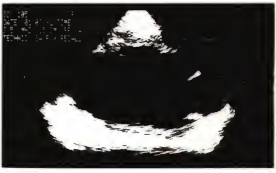

DISCUSSION

Left ventricular responses to aortic insufficiency (AI) remain a complex physiologic and clinical problem. Although left ventricular adaptations to a chronic volume overload induced by AI are characterized by alterations in left ventricular dimensions, volume, wall thickness and stress, the sequence and timing of these physiologic changes are not well documented. It remains unclear as to whether left ventricular muscle function, as evaluated by a variety of isovolumic and ejection phase indices, is altered by aortic insufficiency. Also, no data clearly define whether a recognizable sequence of changes in function can be associated with the duration of the disease. Several clinical studies on aortic insufficiency have reported the alterations in left ventricular dimensions and wall thickness, and attempted to evaluate left ventricular function (53, 84-86). There have been other clinical reports on AI which described sequential changes in the left ventricle in symptomatic patients (87-89) or following aortic valve replacement (50,54,57). These clinical studies are difficult to interpret since marked variability in the duration of volume overload must exist in the patients studied.

An experimental model which simulates the chronic volume overload produced by AI should offer the advantage of known duration and magnitude of volume overload. In vivo animal models of volume overload

can be categorized according to techniques used in creating the overload: arteriovenous fistula (51,52,59,81,90), complete heart block (26,91,92) and aortic valve perforation (55,59). The arteriovenous fistula model has provided insight into both ultrastructural and physiologic adaptations to volume overload (93,94). But it appears that a model which creates overload by aortic valve perforation is more analagous to the human disease of aortic insufficiency. Here the defect is at the sub-coronary level and factors affecting alterations of left ventricular loading and coronary perfusion should operate at this level. Accordingly, this study used an aortic valve perforation model of aortic insufficiency in order to serially evaluate the left ventricular response to volume overload.

Left ventricular dilatation detected by echocardiographically measured increases in left ventricular minor axis end diastolic (EDD) and end systolic dimensions (ESD) occurred as early as one week after AI was created. Left ventricular dimensions continued to increase rapidly during the first two months after creation of AI. Thereafter, these dimensions increased at a rate comparable to that observed in the Control group. A similar pattern of left ventricular dilatation was detected using serial angiographic assessment of left ventricular volume. Left ventricular volume was significantly increased three months after creation of AI and then increased at a slower rate during the rest of the study. Two dimensional echocardiography at twenty-four months of age confirmed these findings by demonstrating that left ventricular volume was approximately 60-100% greater in the AI group.

A moderate degree of left ventricular hypertrophy occurred in the AI group. Hypertrophy was demonstrated by an increased rate of thickening of both left ventricular posterior (0.24 mm/mo.) and septal walls (0.18 mm/mo.). Hypertrophy appeared to be an adaptation to an increase in left ventricular circumferential wall stress which was documented three months after creation of AI. The increase in wall stress was also associated with an R/h ratio which remained elevated from one week through three months after AI. Wall stress appeared to normalize by eight months after AI as the left ventricular posterior and septal walls continued to thicken. Further evidence of left ventricular hypertrophy was demonstrated by a 20% increase in left ventricular mass as determined by 2D echocardiography.

There was a significant decrease in left ventricular systolic function detected as early as one month after creation of AI. Both peak normalized rate of left ventricular shortening (peak -dD/dt/D) and shortening fraction demonstrated this early depression in function. These indices of left ventricular function continued to decrease in the AI group throughout the study at a rate of 0.11 sec^{-1}/mo. for peak -dD/dt/D and 0.77%/mo. for shortening fraction. These data are consistent with angiographic, 2D echocardiographic and ventricular-loading study data which all demonstrated a depression of left ventricular systolic function in the AI group when compared to the Controls. Although angiographic ejection fraction was normal in the AI group three months after creation of AI, it was significantly decreased eight months after AI. Also at eight months after AI, a 30% depression in left ventricular systolic function was demonstrated in the AI group

when aortic pressure was increased with phenylephrine. Two dimensional echocardiographic evaluation of ejection fraction at twenty-four months of age (twenty months after AI) also demonstrated a decrease in left ventricular function.

Data concerning alterations in left ventricular diastolic function are less conclusive. Serial echocardiography demonstrated an early (one month after AI) and continued decrease in the peak normalized rate of left ventricular filling (peak +dD/dt/D). However, analysis of the end diastolic pressure-dimension relation obtained during the ventricular-loading study did not reveal any decrease in left ventricular diastolic compliance. Further investigation of diastolic properties of the left ventricle is needed to clarify serial changes which occur during chronic AI.

There are several limitations to this study which must be considered when evaluating these data. All conclusions inferred from this study are qualified by the fact that only eleven animals were studied. Because of the small number of animals, dictated by the length and costs of this study, only conservative statistical analyses were performed. Some factors contributing to variability in serial echocardiographic data were variability in heart rate, time of day and environmental conditions when the data were obtained. Reproducibility of serial echocardiographic measurements have been tested in several clinical trials (87, 95-98), but not in animal models. Martin and Fieller (96) examined the variability of several echocardiographic parameters in five normal human subjects. They reported the coefficient of variation for end diastolic and end systolic dimensions

were 3.4 and 3.3% respectively. They also predicted the magnitude of change with a 95% probability of being true change was 3.9 mm for EDD, 2.7 mm for ESD, 6.2% for shortening fraction and 0.22 circ/sec for mean Vcf. Felner et al. (97) used a variance component analysis and reported the reproducibility of serial left ventricular dimensions were 3-4%. Others have reported that the variability for repeated measurements of shortening fraction ranged up to 10% (87,98). These data confirm the validity of using serial echocardiography in a reproducible fashion in human subjects, but are not directly applicable to animal models such as the present study. Reproducibility of serial echocardiographic data in the present study demonstrate variability similar to that reported in clinical studies. In particular, the coefficient of variation for left ventricular dimensions were 2-4%, for wall thickness and shortening fraction were 8%, and for the peak rates of dimension change were 20%. Even though the coefficient of variation for peak rate of LV shortening was approximately 20%, observations concerning changes in LV systolic function were considered valid because similar changes occurred in shortening fraction which had less variability.

Serial angiographic, hemodynamic, wall stress and ventricular-loading study data must also be interpreted with caution because these data were obtained while the animals were anesthetized and lying in a lateral position. Although conclusions based on these data should be valid because they are compared to a Control group, these results may be different when compared to a conscious animal with complete reflex activity. The end diastolic dimension of the AI group

at twelve months of age demonstrated that EDD was larger when the animals were anesthetized and lying down (53.3 $\pm$ 2.6mm) as compared to a conscious and standing position (47.4 $\pm$ 2.2mm). This difference may have been due to alterations in venous return and preload due to position of the animals and anesthesia. Because of variability in degree of anesthesia and reflex activity in these animals, certain trends in serial data were considered important (wall stress data) even though they were not significant at the $p< .05$ level.

Although many studies have evaluated left ventricular responses during experimental aortic insufficiency, there is considerable variability in results reported in the literature. It is difficult to adequately control the degree of left ventricular volume overload using an experimental model. Therefore, it is important to evaluate the degree of volume overload throughout the study period. In this study, the severity of the lesion was quantitated angiographically and was re-evaluated twice during the one year study period. Taylor and Hopkins (59) attempted to quantitate the volume load on the left ventricle on the basis of post-mortem examination of the aortic valve leaflets. They reported that in their dogs, moderate AI was associated with a 5 mm tear of the non-coronary valve leaflet while more severe AI was related to either a longer duration of AI or a larger tear in one valve leaflet. This approach bears an uncertain relationship to the actual severity of AI during life.

Taylor and Hopkins (59) did not observe early left ventricular dilatation after perforating an aortic valve leaflet. Their inability to detect early dilatation may have been due partly to their

calculations of left ventricular volume from assessment of passive pressure-volume curves of anoxia-arrested ventricles. However, Belenkie and Rademaker (55), who used an echocardiographic evaluation of experimental AI similar to the present study, observed an early increase in left ventricular dimensions. Only one experimental study which used a fistula model of volume overload provided pre-fistula data (52). This data demonstrated a slightly less rapid rate of left ventricular dimension increase for one month when compared to the present study.

Left ventricular hypertrophy has been the most common observation made in the study of aortic insufficiency (5-8,52,54,56-59,81,88-94). However, there is little agreement concerning the time interval from onset of AI to the development of hypertrophy and whether volume overload hypertrophy is associated with any change in left ventricular function. This controversy may be due partly to differences in experimental models or patients evaluated and techniques used to assess left ventricular hypertrophy and function. It has been hypothesized that the stimulus for left ventricular hypertrophy (eccentric hypertrophy) is an increase in left ventricular wall stress (50-57,84,85,87-89,91-94,99-107). Although an increase in left ventricular wall stress in patients with aortic insufficiency has been reported (79,108-110), there has not been any study, besides the present one, which has evaluated serial changes in wall stress during AI. Grossman et al. (110) has suggested that hypertrophy may develop to normalize systolic but not diastolic wall stress. An increase in systolic tension development during aortic insufficiency resulted in

myocardial fiber thickening sufficient to return systolic stress to normal. In contrast, increased diastolic or resting tension resulted in myocardial fiber elongation which helped maintain adequate systolic ejection of the volume overload, but did not normalize diastolic wall stress (110). These results are similar to the changes in wall stress observed in the present study. The ratio of left ventricular chamber radius to posterior wall thickness, R/h ratio, has been used to reflect the degree to which the LV muscle mass is appropriate for a given chamber volume (54,111). Several studies have demonstrated that the R/h ratio is within normal limits in patients with chronic aortic insufficiency (54,110,111). The present study demonstrated that normalization of the R/h ratio occurred within four months after the onset of experimental AI.

The observaton of early left ventricular dilatation in the present study supports the hypothesis that left ventricular sarcomeres may be maximally stretched as early as one week after initiation of a volume overload (56,94,95). Thereafter, an increase in number of myocardial fibers, both in parallel and in series, may occur as left ventricular dilatation continues (56,93,112). It is thought that hypertrophy is probably related to both the severity and the duration over which the volume overload exists (54,87). Clinical observations in patients which examined the relationship between age of the patient and clinical disability inferred similar conclusions (89). Thus, it appears that compensatory mechanisms consisting of left ventricular dilatation and hypertrophy are important physiologic adaptations of the left ventricle to aortic insufficiency.

Many studies have evaluated left ventricular function after onset of AI with conflicting results (26,27,29,30,49-55,84-87,90-92). However, there is considerable variability in the methodology of these reports. Experimental models employing an aorto-caval fistula use the animals as their own controls and compare pre-fistula to one month post-fistula data (52). Other studies have compared one week fistula to two month fistula data (51,81). Such studies do not provide longitudinal observations of control animals and the possibility of time-related changes in the experimental group are subject to question. It is also difficult to assess clinical investigations of left ventricular function if the actual onset of AI is unknown and the grouped patient data can only be compared to age-matched normals (57, 85,87,113). Only one other study (55) examined changes in left ventricular function during AI using both a control and experimental group and did not demonstrate a significant difference in function as measured by shortening fraction. This study raises several methodological questions inasmuch as there was no estimate of either degree of aortic valve damage or severity of AI created. Also, there were no data which demonstrated persistence of experimental AI throughout the eight month study.

In the present study, left ventricular function was depressed in the AI group when compared to the Control group. This was demonstrated by serial echocardiographic measurements of shortening fraction and peak -dD/dt/D, and serial angiographic and 2D echocardiographic evaluation of ejection fraction. Although it is appropriate to question the use of M-mode echocardiographic measurements as an

accurate reflection of left ventricular function in an animal model, the validity of SF and peak -dD/dt/D have been previously established (114-117). Peak -dD/dt/D has correlated well with isovolumic indices of contractility (114-116), angiographically measured velocity of circumferential fiber shortening (118-119) and hemodynamic measurements of the maximal first derivative of left ventricular pressure (120,121). Another question concerns the ability of an "ice-pick" view of the ventricular minor axis using M-mode echocardiography to reflect global ventricular performance. Badke and Covell (90) have reported on regional differences in the extent of left ventricular dilatation and function during a chronic volume overload. Using an aorto-caval fistula model, their data demonstrated an increase in shortening fraction after two weeks of volume overload, with the greatest percent increase observed in the apical portion of the ventricle. However, forty days after creation of the fistula, they observed that left ventricular function started to decrease in all regions which is consistent with the data from the present study.

A hypothesis supporting the depression in left ventricular function observed in the present experimental model of AI can be partially based upon reported data concerning coronary hemodynamics during AI. Feldman et al. (46) used an experimental model of acute AI to demonstrate that coronary flow reserve, measured by the hyperemic response to a transient coronary artery occlusion, was reduced with AI. This study also demonstrated that diastolic coronary flow was reduced and implied that the combination of reduced coronary reserve and diastolic blood flow might decrease subendocardial perfusion. Segal et

al. (122) examined one hundred cases of severe AI and reported that angina was present in 50% of the patients. They hypothesized that angina due to myocardial ischemia might be due to either lowering of aortic diastolic pressure with an associated decrease in coronary flow, a suction effect of regurgitant aortic flow on coronary flow, or relative ischemia related to left ventricular hypertrophy. Mizutani has reported evidence for backward flow during diastole and reduced coronary systolic flow during acute experimental AI with regurgitant fractions greater than 70% (123). A reversal in direction of coronary flow during diastole has been reported by others (46,124). Badke et al. (125) examined coronary flow distribution using an aorto-caval fistula model of volume overload. These authors attempted to separate the effects of hypertrophy from alterations in aortic pressure on the resultant coronary blood flow. They demonstrated that myocardial perfusion was normal at rest, but subendocardial underperfusion occurred during exercise in six dogs with the fistula. Also, minimal mean coronary vascular resistance measured during exercise with an infusion of adenosine was normal in these dogs. Effects of hypertrophy alone were evaluated by repairing the fistula. Post-fistula results demonstrated that both subendocardial perfusion and minimal mean coronary resistance were normal. Although these results might appear to conflict with the finding of Feldman et al. (46) that coronary reserve was diminished with AI, there are differences in experimental model, hemodynamic parameters and techniques used in estimating coronary vascular reserve which makes the comparison unjustified.

The volume overload produced by aortic insufficiency initially causes left ventricular dilatation and an increase in left ventricular wall stress. The increase in wall stress may be a stimulus for replication of myocardial sarcomeres, fiber elongation and eccentric hypertrophy. Whether there is an associated hyperplasia of connective tissue elements to increase coronary vascular channels is unknown (99-106). Although total myocardial oxygen consumption appears to be normal in the resting state(126,127), there is no data reflecting oxygen demands in different layers of the myocardium. It is possible that an increase in endocardial wall stress associated with AI may cause an increase in subendocardial oxygen demands resulting in relative subendocardial ischemia. Relative subendocardial ischemia (32,46,125) and decreased left ventricular ejection fraction (59,60,85,86,128,129) have been reported both in animals and patients with AI during periods of stress. Even without a decrease in coronary perfusion pressure (aortic diastolic pressure), the decrease in left ventricular function observed in the present study may be due in part to a redistribution of myocardial blood flow to epicardial regions with associated subendocardial ischemia.

The possibility that left ventricular function may be depressed in chronic aortic insufficiency has important implications in clinical management of patients with AI and timing of surgery for aortic valve replacement. Gault et al. (50) reported that four patients with depressed preoperative myocardial contractile indices did not demonstrate postoperative improvement in left ventricular function despite correction of the volume overload. Since this original report,

several studies have examined postoperative myocardial performance as well as preoperative indices to indicate appropriate timing for aortic valve replacement (54, 130-137). Henry et al. (132,133) has proposed the use of an end systolic dimension of greater than 55 mm to indicate that surgical intervention is appropriate. Gaasch et al. and others have reported that the preoperative R/h ratio can help predict which patients will improve postoperatively (130,137), while others have used the left ventricular ejection fraction at rest and during exercise for the same purpose (54,60,84,86,113,128,129,131). The recent report by Acar et al. (136) highlighted the importance of finding a sensitive index of left ventricular contractile function and a reliable preoperative indicator of postoperative myocardial performance. They retrospectively examined an eight year period following aortic valve replacement in 248 patients with aortic stenosis and 126 with aortic insufficiency. Discounting perioperative mortality, the aortic insufficiency group had an eight year survival rate of only 61% compared to 84% for the aortic stenosis patients despite the fact that the AI group was on the average fourteen years younger (136).

The present study has outlined a physiologic sequence of left ventricular adaptations to a chronic volume overload created by aortic insufficiency. Despite its limitations, this study has provided some important insights in the evaluation of left ventricular responses to aortic insufficiency in a chronic, conscious animal model because the onset, severity and duration of AI were known. Left ventricular responses to aortic insufficiency in this experimental model were early left ventricular dilatation followed by a gradual eccentric hypertrophy

and a trend towards normalization of circumferential wall stress. However, left ventricular function decreased fairly rapidly after onset of AI and did not demonstrate any improvement despite left ventricular hypertrophy and normalization of wall stress. Whether these results bear any relationship to the pathophysiologic course of the human disease remains to be investigated.

APPENDIX

PRINCIPLES OF ULTRASOUND

In order to understand the concepts and techniques of echocardiography, it is necessary to review the basic principles of ultrasound and its applications to ultrasonographic imaging of the heart. Ultrasound is defined as having a frequency greater than 20,000 cycles per second (Hz), which is above the audible range for humans. Actually, the range of ultrasound used for diagnostic purposes is between one and five million cycles per second (1-5 MHz). A sound wave is a series of compressions and rarefactions. The combination of a compression and rarefaction is a cycle and the distance between peak compression of one cycle and the next represents the wavelength. The frequency represents the number of cycles per second and the velocity is the speed at which sound waves travel through a particular medium. Therefore, the resulting relationship that the velocity of sound is equal to the frequency times the wavelength indicates that the higher the frequency, the smaller the wavelength will be. The velocity of sound is dependent on the density of the medium and is approximately 1,540 meters per second for soft human tissue. The pattern and speed which sound travels through a medium is referred to as the acoustic impedance of that medium. The acoustic impedance is defined as the

density of the medium times the velocity of sound in that medium. A sound wave travels essentially in a straight path through a homogenous medium. When this sound wave or beam reaches an interface of two media with different acoustic impedances, a portion of the wave is reflected and refracted in a manner dependent on the angle of incidence at which the sound beam hits the interface. The underlying principle of all ultrasound techniques is that ultrasound is reflected at an interface of media with different acoustic impedances. Table 9 provides data on the velocity of sound, density and acoustic impedance of various media important in medical applications (138).

The detection of reflected waves are based upon the principle of the piezoelectric effect. The piezoelectric effect is described as the mechanical strain on a material produced when an electric field is applied. The amount of strain is proportional to the intensity of the electric field. This effect is reversible meaning that when this material is struck by a sound wave and strained, it produces an electrical impulse. Commercial transducers used in echocardiography use either barium titanate or lead zirconate titanate as the piezoelectric element (139). Typically, the thickness of the piezoelectric element is one-fourth of the wavelength of the transmitted sound frequency. The reflection of ultrasound by an interface is dependent not only on the acoustic impedance ratio of the two media and the angle of incidence, but also on the thickness of the differing media or structure. Reflection of ultrasound will only occur if the thickness of the presenting structure is at least one fourth the wavelength of the ultrasound (139). Ultrasound having a higher

TABLE 9
ACOUSTICAL CHARACTERISTICS OF VARIOUS MEDIA

Medium	Velocity (meter/sec)	Density (g/cm^3)	Impedance ($g/cm^2/sec$) x 10^{-5}
Air	331	0.0012	0.0004
Water	1480	1.00	1.48
Blood	1570	1.03	1.61
Muscle	1585	1.07	1.70
Bone	4080	1.91	7.80

Source: (138)

frequency and therefore a shorter wavelength can reflect sound from smaller objects and thus provide a greater resolving power. The typical resolution of an echocardiographic transducer is between one and two wavelengths. In other words, using a 3.5 MHz transducer on soft tissue having a velocity of sound of 1,540 m/sec, the wavelength is 0.44 mm and the range of resolution is 0.5 - 1.0 mm. It should also be apparent that since high frequency ultrasound is reflected by smaller interfaces in a nonhomogenous media such as human tissue, there is less ultrasonic energy available for deeper penetration. Therefore, as the frequency and resolving power of the ultrasound increases, the penetration of the beam decreases. Similarly, the amount of absorption and scattering which also increase with increasing ultrasound frequency decrease the depth of penetration of the beam.

M-Mode Echocardiography

Most M-mode echocardiograph transducers transmit sound for approximately one microsecond and receive sound for the next 999 microseconds. Therefore, one thousand complete transmit-receive cycles occur each second. The sound transmitted from a single pulse can travel through the thorax and its echoes received by the transducer before the next pulse, thereby eliminating any interference from subsequent sound waves (140). Assuming a constant velocity for sound in soft tissue, the time for ultrasound to travel through the tissue until it hits a reflecting surface and then back to the transducer gives the distance of the transducer from the reflecting surface(141; Figure 38). Once the returning echo is received and transduced into an electrical

Figure 38. An idealized M-mode echocardiogram displaying the depth of reflected structures as a function of time.

Source: (141) reprinted with permission of Merck, Sharp and Dohme.

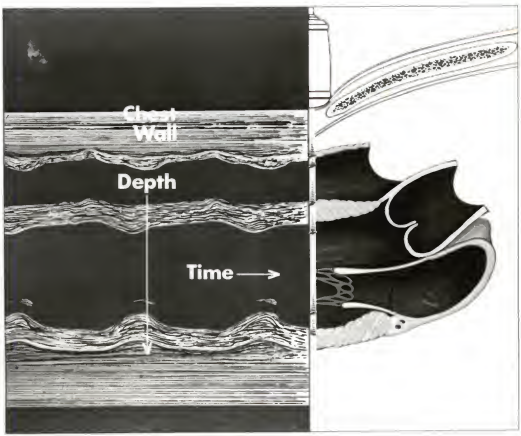
Chest
Wall
Depth
Time

signal, it is electronically processed before being displayed on an oscilloscope. The signal can be displayed by amplitude modulation known as A-mode or converted to an intensity or brightness modulation known as B-mode. When this B-mode echo is displayed as a function of time, the echocardiograph can show motion of the reflecting surfaces. This is known as motion or M-mode echocardiography (141; Figure 39).

The ultrasonic beam transmitted by the piezoelectric element in a transducer propagates essentially in a parallel manner through a medium for a certain distance and then begins to diverge. The part of the beam which is parallel is known as the near field and the divergent zone is the far field. Ultrasound works best when the reflecting surfaces of interest are located in the near field because the reflecting surfaces are more nearly perpendicular to the ultrasound beam and thus reflect echoes of greater intensity. The length of the near field is determined by the following relationship: near field length equals the transducer radius squared (r^2) divided by the wavelength (142). Thus, increasing either the transducer radius or the frequency of ultrasound will increase the length of the near field. For a typical M-mode echo transducer having a radius of 6 mm and a wavelength of 0.44 mm (frequency is 3.5 MHz), the near field length is 88 mm. The angle of divergence of the sound beam in the far field is predicted from the relationship: Sin $\emptyset$ equals 1.22 multiplied by the wavelength divided by the transducer diameter (140). It is difficult to increase the size of the transducer head because this is limited by the ability to direct the transducer and its ultrasound beam through an intercostal space. Furthermore, the tradeoff between increasing the

Figure 39. An idealized M-mode echocardiogram displaying the depth of reflected cardiac structures as a function of time. o(anterior wall of right ventricle); p (interventricular septum); q (left ventricular posterior epicardium); LVIDd (end diastolic dimension); LVIDs (end systolic dimension).

Source: (141) reprinted with permission of Merck, Sharp and Dohme.

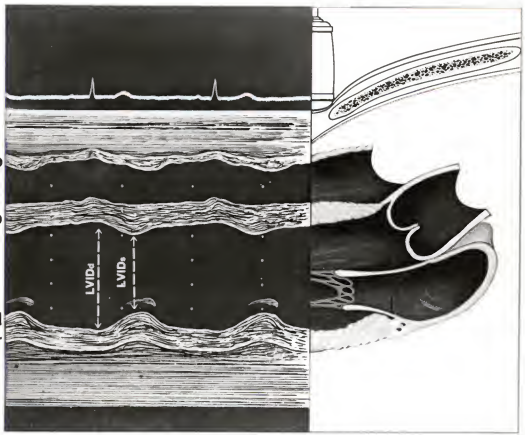
o
p
q
r
LVIDd
LVIDs

frequency and decreasing the penetration of ultrasound has been prevously discussed. Therefore, echocardiographs use either an acoustic lens or an electronic phased array system to focus the ultrasound beam and delay the subsequent divergence.

There are many other types of signal processing which occur before the ultrasound echo is displayed on the oscilloscope or recorded on photographic paper. There is a technique for differentiation or leading-edge enhancement which helps to accentuate individual echoes and also provides some distinction between two echoes which are close together. Secondly, the transducer receiver has the ability to detect echoes over an amplitude range of one to 100,000. For this reason, echocardiographs use logarithmic amplifiers to compress this range into a reasonable output display (139). It was previously discussed that the ultrasound and returning echoes are attenuated as they travel through tissue due to previous reflection, absorption and refraction. The mechanism for enhancing distant echoes and suppressing near field echoes is known as time-gain or depth compensation. These are only a few of the basic adjustments made on the received echo signal before it is displayed as a M-mode echocardiogram.

Two Dimensional Echocardiography

Two dimensional (2D) or cross-sectional echocardiography uses the same B-mode information acquired by the M-mode technique, "freezes" it and then displays this information as the transducer is moved along an imaging plane. If the scan of the imaging plane is done rapidly enough, the display on the oscilloscope becomes a "real-time" or 2D

image of the cross-sectional plane. Two dimensional echo transducers either mechanically or electronically scan through the body to create an imaging plane. One of the major differences between M-mode and 2D techniques is that the 2D image displays the B-mode depth with its direction of origin relative to the transducer. These tomographic images are displayed as a "frozen" frame and most 2D echocardiographs can display 30 frames per second (143). This is in comparison to the M-mode sampling rate of approximately 1,000 per second. Thus, rapidly moving structures such as cardiac valve motion and high frequency vibrations are better observed by M-mode echo. Also, the "ice-pick" view provided by M-mode echo allows for a more accurate quantitation of the depth and thickness of structures present in this view. However, the advantages of 2D imaging include a better assessment of the size and shape of cardiac structures and information concerning the anatomical relationships of structures. It is the ability to use both M-mode and 2D echocardiography together which can provide a relatively accurate non-invasive evaluation of cardiac size, shape and function.

REFERENCES

1. Hodgkin, T. On retroversion of the valves of the aorta. London Medical Gazette 3:433, 1828.

2. Corrigan, D.J. On permanent patency of the mouth of the aorta, or inadequacy of the aortic valves. Edinburgh Medical and Surgical Journal 37:225, 1832.

3. Stewart, H.A. Experimental and clinical investigation of the pulse and blood pressure changes in aortic insufficiency. Archives of Internal Medicine 1:102, 1908.

4. MacCallum, W.G. On the teaching of pathological physiology. Johns Hopkins Hospital Bulletin 17:251, 1906.

5. Stewart, H.A. An experimental contribution to the study of cardiac hypertrophy. Journal of Experimental Medicine 13:187, 1911.

6. Herrmann, G.R. Experimental heart disease: The effect of experimental aortic regurgitation on the heart weights. American Heart Journal 1:485, 1926.

7. Bazett, H.C. and Sands, J. An experimental study of chronic aortic regurgitation in dogs. Journal of Clinical Investigation 3:65, 1926.

8. Eyster, J.A.E., Meek, W.J. and Hodges, F.J. Cardiac changes subsequent to experimental aortic lesions. Archives of Internal Medicine 39:536, 1927.

9. Wiggers, C.J. Reflex vasodilation is not the cause of the collapsing pulse of aortic insufficiency. Proceedings of the Society for Experimental Biology and Medicine 12:55, 1914.

10. Wiggers, C.J. Studies on the pathological physiology of the heart. Archives of Internal Medicine 16:132, 1915.

11. MacCallum, W.G. The changes in the circulation in aortic insufficiency. Johns Hopkins Hospital Bulletin 22:197, 1911.

12. Wiggers, C.J., Thiesen, H. and Williams, H.A. Further observations of experimental aortic insufficiency: Cinematographic studies of changes in ventricular size and in left ventricular discharge. Journal of Clinical Investigation 9:215, 1930.

13. Wiggers, C.J. The magnitude of regurgitation with aortic leaks of different sizes. Journal of the American Medical Association 97:1359, 1931.

14. Lewis, T. and Drury, A.N. Observations relating to arterio-venous aneurism:Circulatory manifestations in clinical cases with particular references to arterial phenomena of aortic regurgitation. Heart 10:301, 1923.

15. Dock, W. and O'Hara, J.J. A rubber-opposed haemodromograph used to measure reflux in aortic insufficiency. Proceedings of the Society for Experimental Biology and Medicine 25:706, 1928.

16. Gladstone, S.A. A few observations on the haemodynamics of the normal circulation; and the changes which occur in aortic insufficiency. Johns Hopkins Hospital Bulletin 44:83, 1928.

17. Wiggers, C.J. and Maltby, A.B. Further observations on experimental aortic insufficiency: Hemodynamic factors determining the characteristic changes in aortic and ventricular pressure pulses. American Journal of Physiology 97:689, 1931.

18. Wood, E.H., Woodward, E.,Jr., Swan, H.J.C. and Ellis, F.H.,Jr. Detection and estimation of mitral regurgitation by indicator-dilution technics. Journal of Clinical Investigation 35:745, 1956.

19. Braunwald, E. and Morrow, A.G. Method for detection and estimation of aortic regurgitant flow in man. Circulation 17:505, 1958.

20. Armelin, E., Michaels, L., Marshall, H.W., Donald, D.E., Cheesman, R.J. and Wood, E.H. Detection and measurement of experimentally produced aortic regurgitation by means of indicator-dilution curves recorded from the left ventricle. Circulation Research 12:269, 1963.

21. Malooly, D.A., Donald, D.E., Marshall, H.W. and Wood, E.H. Assessment of an indicator-dilution technic for quantitating aortic regurgitation by electromagnetic flowmeter. Circulation Research 12:487, 1963.

22. Sandler,H. Dodge, H.T., Hay, R.E. and Rackley, C.E. Quantitation of valvular insufficiency in man by angiocardiography. American Heart Journal 65:501, 1963.

23. Arcilla, R.A., Agustsson, M.H., Steiger, Z. and Gasul, B.M. Angiocardiographic sign of aortic regurgitation. Circulation 23:269, 1961.

24. Hunt., Baxley, W.A., Kennedy, J.W., Judge, T.P, Williams, J.E. and Dodge, H.T. Quantitative evaluation of cineaortography in the assessment of aortic regurgitation. American Journal of Cardiology 31:696, 1973.

25. Newman, M.M., Bay, E.B., Lokin, A. and Adams, W.E. Electromagnetic measurement of aortic blood flow in the presence of artificial aortic insufficiency. Surgical Forum 1:304, 1950.

26. Welch, G.H., Braunwald, E. and Sarnoff, S.J. Hemodynamic effects of quantitatively varied experimental aortic regurgitation. Circulation Research 5:546, 1957.

27. Schenk, W.G., Jr., Portin, B.A., Leslie, M.B. and Andersen, M.N. Hemodynamics of experimental aortic insufficiency. Annals of Surgery 150:104, 1959.

28. Weldon, C.S. and Cooper, T. Aortic flow characteristics in experimental aortic insufficiency. Surgical Forum 9:325, 1959.

29. Schenk, W.G.,Jr., Menno, A.D. and Martin, J.W. Hemodynamics of chronic experimental aortic insufficiency. Annals of Surgery 154:295, 1961.

30. Nolan, S.P. and Muller, W.H.,Jr. Comparison of acute and chronic experimental aortic insufficiency. Surgical Forum 13:210, 1962.

31. Morrow, A.G., Brawley, R.K. and Braunwald, E. Effects of aortic regurgitation on left ventricular performance. Direct determinations of aortic blood flow before and after valve replacement. Circulation 31(Suppl.I):80, 1965.

32. Brawley, R.K. and Morrow, A.G. Direct determinants of aortic blood flow in patients with aortic regurgitation. Effects of alterations in heart rate, increased ventricular preload or afterload, and isoproteronol. Circulation 35:32, 1967.

33. Mennel, R.G., Joyner, C.R., Thompson, P.D., Pyle, R.R. and MacVaugh, H.,III. The preoperative and operative assessment of aortic regurgitation. Cineaortography vs. electromagnetic flowmeter. American Journal of Cardiology 29:360, 1972.

34. Denison, A.B., Spencer, M.P. and Green, H.D. A square-wave electromagnetic flowmeter for application to intact blood vessels. Circulation Research 3:39, 1955.

35. Hilder, F.J., Pierson, W.R. and Barold, S.S. Isotope quantitation of aortic insufficiency compared to cineangiography in man. Annals of Thoracic Surgery 8:85, 1969.

36. Rigo, P., Alderson, P.O., Robertson, R.M., Becker. L.C. and Wagner, H.N. Measurement of aortic and mitral regurgitation by gated blood pool scans. Circulation 60:306, 1979.

37. Sorenson, S.G., MGroves, B.M., O'Rourke, R.A. and Chaudhuri, T. Noninvasive quantitation of valvular regurgitation by gated radionuclide angiography. Journal of Nuclear Medicine 20:626, 1979(abstr.).

38. Nolan, S.P., Fisher, R.D., Dixon, S.H.,Jr. and Morrow, A.G. Quantification of aortic regurgitation with a catheter tip velocitometer. Surgery 65:876, 1969.

39. Nichols, W.W., Pepine, C.J., Conti, C.R., Christie, L.G. and Feldman, R.L. Quantitation of aortic insufficiency using a catheter-tip velocity transducer. Circulation 64:375, 1981.

40. Smith, F.M., Miller, G.H. and Graber, V.C. The relative importance of the systolic and the diastolic blood pressure in maintaining the coronary circulation. Archives of Internal Medicine 38:108, 1926.

41. Green, H.D. The coronary blood flow in aortic stenosis, in aortic insufficiency and in arterio-venous fistula. American Journal of Physiology 115:94, 1936.

42. Wegria, R., Muelheims, G., Golub, J.R., Jreissaty, R., and Nakano, J. Effect of aortic insufficiency on arterial blood pressure, coronary blood flow and cardiac oxygen consumption. Journal of Clinical Investigation 37:471, 1958.

43. West, J.W., Wendel, H. and Foltz, E.L. Effects of aortic insufficiency on circulatory dynamics of the dog. Circulation Research 7:685, 1959.

44. Griggs, D.M.,Jr. and Chen, C.C. Coronary hemodynamics and regional myocardial metabolism in experimental aortic insufficiency. Journal of Clinical Investigation 53:1509, 1974.

45. Falsetti, H.L., Carroll, R.J. and Cramer, J.A. Total and regional myocardial blood flow in aortic regurgitation. American Heart Journal 97:485, 1979.

46. Feldman, R.L., Nichols, W.W., Pepine, C.J. and Conti, C.R. Influence of aortic insufficiency on the hemodynamic significance of a coronary artery narrowing. Circulation 60:259, 1979.

47. Ferguson, T.B., Gregg, D.E. and Shadle, O.W. Effect of blood and saline infusion on cardiac performance in normal dogs and with arteriovenous fistulas. Circulation Research 2:565, 1954.

48. Brockman, S.K. Cardiodynamics of complete heart block. American Journal of Cardiology 16:72, 1965.

49. Urschel, C.W., Covell, J.W., Sonnenblick, E.H., Ross, J., Jr. and Braunwald, E. Myocardial mechanics in aortic and mitral valvular regurgitation: The concept of instantaneous impedance as a determinant of the performance of the intact heart. Journal of Clinical Investigation 47:867, 1968.

50. Gault, J.H., Covell, J.W., Braunwald, E. and Ross, J. Jr. Left ventricular performance following correction of free aortic regurgitation. Circulation 42:773, 1970.

51. Ross, J. Jr. and McCullagh,W.H. Nature of enhanced performance of the dilated left ventricle in the dog during chronic volume overloading. Circulation Research 30:549, 1972.

52. LeWinter, M.M., Engler, R.L. and Karliner, J.S. Enhanced left ventricular shortening during chronic volume overload in conscious dogs. American Journal of Physiololgy 238:H126, 1980.

53. McDonald, I.G. Echocardiographic assessment of left ventricular function in aortic valve disease. Circulation 53:860, 1976.

54. Schuler, G., Peterson, K.L., Johnson, A.D., Francis, G., Ashburn, W., Dennish, G, Daily, P.O. and Ross, J., Jr. Serial noninvasive assessment of left ventricular hypertrophy and function after surgical correction of aortic regurgitation. American Journal of Cardiology 44:585, 1979.

55. Belenkie, I. and Rademaker, A. Acute and chronic changes after aortic valve damage in the intact dog. American Journal of Physiology 241:H95, 1981.

56. Ross, J. Jr. Adaptations of the left ventricle to chronic volume overload. Circulation Research 35(Suppl. II):64, 1974.

57. Fischl, S.J., Gorlin, R. and Herman, M.V. Cardiac shape and function in aortic valve disease: Physiologic and clinical implications. American Journal of Cardiology 39:170, 1977.

58. Taylor, R.R., Covell, J.W. and Ross, J. Jr. Left ventricular function in experimental aorto-caval fistula with circulatory congestion and fluid retention. Journal of Clinical Investigation 47:1333, 1968.

59. Taylor, R.R. and Hopkins, B.E. Left ventricular response to experimentally induced chronic aortic regurgitation. Cardiovascular Research 6:404, 1972.

60. Bolen, J.L., Holloway, E.L., Zener, J.C., Harrison, D.C. and Alderman, E.L. Evaluation of left ventricular function in patients with aortic regurgitation using afterload stress. Circulation 53:132, 1976.

61. Sellers, R.D., Levy, M.J., and Amplatz, K. Left retrograde cardioangiography in acquired cardiac disease. Technic indications and interpretations in 700 cases. American Journal of Cardiology 14:437, 1964.

62. Upton, M.T. and Gibson, D.G. The study of left ventricular function from digitized echocardiograms. Progress in Cardiovascular Diseases 20:359, 1978.

63. Dodge, H.T., Sandler, H., Ballew, D.W. and Lord, J.D.,Jr. The use of biplane angiocardiography for the measurement of left ventricular volume in man. American Heart Journal 60:762, 1960.

64. Bardeen, C.R. Determination of the size of the heart by means of x-rays. American Journal of Anatomy 23:423, 1918.

65. Rackley, C.R., Dodge, H.T., Coble, Y.D.,Jr. and Hay, R.E. A method for determining left ventricular mass in man. Circulation 29:666, 1964.

66. Geiser, E.A. and Bove, K.E. Calculation of left ventricular mass and relative wall thickness. Archives of Pathology 97:13, 1974.

67. Dodge, H.T., Hay, R.E. and Sandler, H. An angiocardiographic method for directly determining left ventricular stroke volume in man. Circulation Research 11:739, 1962.

68. Sandler, H. and Dodge, H.T. The use of single plane angiocardiograms for calculation of left ventricular volume in man. American Heart Journal 75:325, 1968.

69. Greene, D.G., Carlisle, R., Grant, C. and Bunnell, I.L. Estimation of left ventricular volume by one-plane cineangiography. Circulation 35:61, 1967.

70. Bentivoglio, L.G., Griffith, L.D., Cuesta, A.J. and Geczy, M. Radiographic evaluation of formulas for left ventricular volume using canine casts. Journal of Applied Physiology 33:365, 1972.

71. Bentivoglio, L.G., Cuesta, A.J., Griffith, L.D. and Geczy, M. Evaluation of single plane angiography for left ventricular volume in the intact dog. Cardiovascular Research 10:283, 1976.

72. Millar, H.D. and Baker, L.E. A stable ultraminiature catheter-tip pressure transducer. Medical and Biological Engineering 11:86, 1973.

73. Nichols, W.W. and Walker, W.E. Experience with the Millar PC-350 catheter-tip pressure transducer. Biomedical Engineering 9:58, 1974.

74. Huisman, R.M., Sipkema, P., Westerhof, N. and Elzinga, G. Comparison of models used to calculate left ventricular wall force. Medical and Biological Engineering and Computing 18:133, 1980.

75. Sandler, H. and Dodge, H.T. Left ventricular tension and stress in man. Circulation Research 13:91, 1963.

76. Falsetti, H.L., Mates, R.E., Grant, C., Greene, D.G. and Bunnell, I.L. Left ventricular wall stress calculated from one-plane cineangiography. Circulation Research 26:71, 1970.

77. Mirsky, I. Left ventricular stresses in the intact human heart. Journal of Biophysics 9:189, 1969.

78. Gabe, I.T., Gault, J.H., Ross, J.Jr., Mason, D.T., Mills, C.J., Shillingford, J.P. and Braunwald, E. Measurement of instantaneous blood flow velocity and presuure in conscious man with a catheter-tip velocity probe. Circulation 40:603, 1969.

79. Nichols, W.W., Pepine, C.J., Conti, C.R., Christie, L.G. and Feldman, R.L. Evaluation of a new catheter-mounted electromagnetic velocity sensor during cardiac catheterization. Catheterization and Cardiovascular Diagnosis 6:97, 1980.

80. Winer, B.J. Statistical Principles in Experimental Design. McGraw Hill, New York, 1971.

81. McCullagh, W.H., Covell, J.W. and Ross, J.,Jr. Left ventricular dilatation and diastolic compliance changes during chronic volume overloading. Circulation 45:943, 1972.

82. Sabbah, H.N. and Stein, P.D. Pressure-diameter relations during early diastole in dogs. Circulation Research 48:357, 1981.

83. Grossman, W., McLaurin, L.P., Moos, S.P., Stefadouros, M. and Young, D.T. Wall thickness and diastolic properties of the left ventricle. Circulation 49:129, 1974.

84. Johnson, A.D., Alpert, J.S., Francis, G.S., Vieweg, V.R., Ockene, I. and Hagan, A.D. Assessment of left ventricular function in severe aortic regurgitation. Circulation 54:975, 1976.

85. Osbakken, M., Bove, A.A. and Spann, J.F. Left ventricular function in chronic aortic regurgitation with reference to end-systolic pressure, volume and stress relations. American Journal of Cardiology 47:193, 1981.

86. Paulson, W., Bonghner, D.R., Persand, J. and Deuries, L. Aortic regurgitation: Detection of left ventricular dysfunction by exercise echocardiography. British Heart Journal 46:380, 1981.

87. McDonald, I.G. and Jelinek, V.M. Serial m-mode echocardiography in severe chronic aortic regurgitaion. Circulation 62: 1291, 1980.

88. Spagnuolo, M., Kloth, H., Taronta, A., Doyle, E. and Pasternack, B. Natural history of rheumatic aortic regurgitation. Circulation 44:368, 1971.

89. Goldschlager, N., Pfeifer, J., Cohn, K., Popper, R. and Selzer, A. The natural history of aortic regurgitation: A clinical and hemodynamic study. American Journal of Medicine 54:577, 1973.

90. Badke, F.R. and Covell, J.W. Early changes in left ventricular regional dimensions and function during chronic volume overloading in the conscious dog. Circulation Research 45: 420, 1979.

91. Turina, M., Bussmann, W.D. and Krayenbuhl, H.P. Contractility of the hypertrophied canine heart in chronic volume overload. Cardiovascular Research 3:486, 1969.

92. Newman, W.H. Contractile state of hypertrophied left ventricle in long-standing volume overload. American Journal of Physiology 234:H88, 1978.

93. Ross, J.,Jr., Sonnenblick, E.H., Taylor, R.R., Spotnitz, H.M. and Covell, J.W. Diastolic geometry and sarcomere lengths in the chronically dilated canine left ventricle. Circulation Research 28:49, 1971.

94. Spotnitz, H.M. and Sonnenblick, E.H. Structural conditions in the hypertrophied and failing heart. American Journal of Cardiology 32: 398, 1973.

95. Stefadouros, M.A. and Canedo, M.I. Reproducibility of echocardiographic estimates of left ventricular dimensions. British Heart Journal 39:390, 1977.

96. Martin, M.A. and Fieller, N.R.J. Exhocardiography in cardiovascular drug assessment. British Heart Journal 41:536, 1979.

97. Felner, J.M., Blumenstein, B.A., Schlant, R.C., Carter, A.D., Alimurung, B.N., Johnson, M.J., Sherman, S.W., Klicpera, M.W., Kutner, M.H. and Druckner, L.W. Sources of variability in echocardiographic measurements. American Journal of Cardiology 45:995, 1980.

98. Clark, R.D., Korcuska, K. and Cohn, K. Serial echocardiographic evaluation of left ventricular function in valvular disease, including reproducibility guidelines for serial studies. Circulation 62:564, 1980.

99. Linzbach, A.J. Heart failure from the point of view of quantitative anatomy. American Journal of Cardiology 5:370, 1960.

100. Meerson, F.Z. The myocardium in hyperfunction, hypertrophy and heart failure. Circulation Research 25(Suppl. II):1, 1969.

101. Fanburg, B.L. Experimental cardiac hypertrophy. New England Journal of Medicine 282:723, 1970.

102. Zak, R. Cell proliferation during cardiac growth. American Journal of Cardiology 31:211, 1973.

103. Bove, K.E. Myocardial hypertrophy and enlargement. p.30-55, in The Heart, edited by Hurst, J.W. William and Wilkins, Baltimore, 1974.

104. Alpert, N.R., Hamrell, B.B. and Halpern, W. Mechanical and biochemical correlates of cardiac hypertrophy. Circulation Research 35(Suppl. II):71, 1974.

105. Skelton, C.L. and Sonnenblick, E.H. Heterogeneity of contractile function in cardiac hypertrophy. Circulation Research 35 (Suppl. II):83, 1974.

106. Fuster, V., Danielson, M.A., Robb, R.A., Broadbent, J.C., Brown, A.L.,Jr. and Elveback, L.R. Quantitation of left ventricular myocardial fiber hypertrophy and interstitial tissue in human hearts with chronically increased volume and pressure overload. Circulation 55:504, 1977.

107. Wikman-Coffelt, J., Parmley, W.W. and Mason, D.T. The cardiac hypertrophy process. Analyses of factors determining pathological vs. physiological development. Circulation Research 45: 697, 1979.

108. Hood, W.P., Rackley, C.E. and Rolett, E.L. Wall stress in the normal and hypertrophied human left ventricle. American Journal of Cardilogy 22: 550, 1968.

109. Gould, K.L., Lipscomb, K., Hamilton, G.W. and Kennedy, J.W. Relation of left ventricular shape, function and wall stress in man. American Journal of Cardiology 34:627, 1974.

110. Grossman, W., Jones,D. and McLaurin, L.P. Wall stress and patterns of hypertrophy in the human left ventricle. Journal of Clinical Investigation 56:56, 1975.

111. Gaasch, W.H. Left ventricular radius to wall thickness ratio. American Journal of Cardiology 43:1189, 1979.

112. Legato, M. Sarcomerogenesis in human myocardium. Journal of Cellular and Molecular Cardiology 1:425, 1970.

113. Gray, K.E. and Barritt, D.W. Echocardiographic assessment of severity of aortic regurgitation. British Heart Journal 37:691. 1975.

114. Karliner, J.S., Gault, J.H., Eckberg, D., Mullins, C.B. and Ross, J.,Jr. Mean velocity of fiber shortening: A simplified measure of left ventricular myocardial contractility. Circulation 44:323, 1971.

115. Peterson, K.L., Skloven, D., Ludbrook, P., Uther, J.B. and Ross, J.,Jr. Comparison of isovolumic and ejection phase indices of myocardial performance in man. Circulation 49:1088, 1974.

116. Benzig, G., Stockert, J., Nave, E. and Kaplan, S. Evaluation of left ventricular performance: Circumferential fiber shortening and tension. Circulation 49:925, 1974.

117. Fortuin, N.J., Hood, W.P. and Craige, E. Evaluation of left ventricular function by echocardiography. Circulation 46:26, 1972.

118. Cooper, R.H., O'Rourke, R.A., Karliner, J.S., Peterson, K.L. and Leopold, G.R. Comparison of ultrasound and cineangiographic measurements of the mean rate of circumferential fiber shortening in man. Circulation 46:914, 1972.

119. Gibson, D.G. and Brown, D.J. Measurements of peak rates of left ventricular wall movement in man: Comparison of echocardiography with angiography. British Heart Journal 37:677, 1975.

120. Barnes, G.E., Bishop, V.S., Horwitz, L.D. and Kaspar, R.L. The maximum derivatives of left ventricular pressure and transverse internal diameter as indices of the inotropic state of the left ventricle in conscious dogs. Journal of Physiology 235:571, 1973.

121. Gibson, D.G. and Brown, D.J. Assessment of left ventricular systolic function in man from simultaneous echocardiographic and pressure measurements. British Heart Journal 38:8, 1976.

122. Segal, J., Harvey, W.P. and Hufnagel, G. A clinical study of one hundred cases of severe aortic insufficiency. American Journal of Medicine 21:200, 1956.

123. Mizutani, T. A study of coronary circulation in experimental aortic insufficiency with special reference to phasic coronary flow pattern. Japanese Circulation Journal 37:123, 1973.

124. Folts, J.D. and Rowe, G.G. Coronary and hemodynamic effects of temporary acute aortic insufficiency in intact anesthetized dogs. Circulation Research 35:238, 1974.

125. Badke, F.R., White, F.C., LeWinter, M., Covell, J., Andres, J. and Bloor, C. Effects of experimental volume-overload hypertrophy on myocardial blood flow and cardiac function. American Journal of Physiology 241:H564, 1981.

126. Cooper, G., Puga, F.J., Zujko, K.J., Harrison, C.E. and Coleman, H.N. Normal myocardial function and energetics in volume-overload hypertrophy in the cat. Circulation Research 32:140, 1973.

127. Trenouth, R.S., Phelps, N.C. and Neill, W.A. Determinants of left ventricular hypertrophy and oxygen supply in chronic aortic valve disease. Circulation 53:644, 1976.

128. Borer, J.S., Bacharach, S.L., Green, M.V., Kent, K.M., Henry, W.L., Rosing, D.R., Seides, S.F., Johnston, G.S. and Epstein, S.E. Exercise-induced left ventricular dysfunction in symptomatic and asymptomatic patients with aortic regurgitation: Assessment with radionuclide cineangiography. American Journal of Cardiology 42:351, 1978.

129. Dehmer, G.J., Firth, B.G., Hillis, L.D., Corbett, J.R., Lewis, S.E., Parkey, R.W. and Willerson, J.T. Alterations in left ventricular volumes and ejection fraction at rest and during exercise in patients with aortic regurgitation. American Journal of Cardiology 48:17, 1981.

130. Gaasch, W.H., Andrias, C.W. and Levine, H.J. Chronic aortic regurgitation: The effect of aortic valve replacement on left ventricular volume, mass and function. Circulation 58:825, 1978.

131. Borer, J.S., Rosing, D.R., Kent, K.M., Bacharach, S.L., Green, M.V., McIntosh, C.J., Morrow, A.G. and Epstein, S.E. Left ventricular function at rest and during exercise after aortic valve replacement in patients with aortic regurgitation. American Journal of Cardiology 44:1297, 1979.

132. Henry, W.L., Bonow, R.O., Borer, J.S., Ware, J.W., Kent, K.M., Redwood, D.R., McIntosh, C.L., Morrow, A.G. and Epstein, S.E. Observations on the optimum time for operative intervention for aortic regurgitation. I.Evaluation of the results of aortic valve replacement in symptomatic patients. Circulation 61:471, 1980.

133. Henry, W.L., Bonow, R.O., Rosing, D.R. and Epstein, S.E. Observations on the optimum time for operative intervention for aortic regurgitation. II.Serial echocardiographic evaluation of asymptomatic patients. Circulation 61:484, 1980.

134. O'Rourke, R.A. and Crawford, M.H. Editorial: Timing of valve replacement in patients with chronic aortic regurgitation. Circulation 61:493, 1980.

135. Rahimtoola, S.R. Valve replacement should not be performed in all asymptomatic patients with severe aortic incompetence. Journal of Thoracic and Cardiovascular Surgery 79:163, 1980.

136. Acar, J., Luxereau, P., Ducimetiere, P., Cadilhac, M., Jallut, H. and Vahanian, A. Prognosis of surgically treated chronic aortic valve disease. Journal of Thoracic and Cardiovascular Surgery 82:114, 1981.

137. Kumpuris, A.G., Quinones, M.A., Waggoner, A.D., Kanon, D.J., Nelson, J.G. and Miller, R.R. Importance of preoperative hypertrophy, wall stress and end-systolic dimension as echocardiographic predictors of normalization of left ventricular dilatation after valve replacement in chronic aortic insufficiency. American Journal of Cardiology 49:1091, 1982.

138. Bom, N. Principles of ultrasound. p. 14, in Evaluation of Cardiac Function by Echocardiography, edited by Bleifeld, W., Effert,S., Hanrath, P. and Mathey, P. Springer-Verlag, New York, 1980.

139. Feigenbaum, H. Echocardiography. Lea and Febiger, Philadelphia, 1981.

140. Popp, R.L. Echocardiographic assessment of cardiac disease. Circulation 54:538, 1976.

141. Reichek, N. An Echocardiography Primer. Merck, Sharp and Dohme, 1978.

142. Hertz. C.H. Ultrasonic engineering in heart diagnosis. American Journal of Cardiology 19:6, 1967.

143. Popp, R.L., Rubenson, D.S., Tucker, C.R. and French, J.W. Echocardiography: M-mode and two dimensional methods. Annals of Internal Medicine 93:844, 1980.

BIOGRAPHICAL SKETCH

The author was born on December 17, 1954, in Brooklyn, New York. He graduated from H. Frank Carey High School in Franklin Square, New York, in 1972. He attended The Johns Hopkins University in Baltimore, Maryland, and graduated with a B.A. in natural science in 1976. He spent the next two years as a research associate in the Division of Cardiac Surgery at The Johns Hopkins University School of Medicine. He entered the University of Florida in September, 1978, to pursue his graduate education in physiology.

I certify that I have read this study and that in my opinion it conforms to acceptable standards of scholarly presentation and is fully adequate, in scope and quality, as a dissertation for the degree of Doctor of Philosophy.

Wilmer W. Nichols, Chairman
Associate Professor of Physiology

I certify that I have read this study and that in my opinion it conforms to acceptable standards of scholarly presentation and is fully adequate, in scope and quality, as a dissertation for the degree of Doctor of Philosophy.

Daryl D. Buss
Associate Professor of
Veterinary Medicine

I certify that I have read this study and that in my opinion it conforms to acceptable standards of scholarly presentation and is fully adequate, in scope and quality, as a dissertation for the degree of Doctor of Philosophy.

William W. Dawson
Professor of Physiology

I certify that I have read this study and that in my opinion it conforms to acceptable standards of scholarly presentation and is fully adequate, in scope and quality, as a dissertation for the degree of Doctor of Philosophy.

Carl J. Pepine
Professor of Medicine

I certify that I have read this study and that in my opinion it conforms to acceptable standards of scholarly presentation and is fully adequate, in scope and quality, as a dissertation for the degree of Doctor of Philosophy.

Wendell N. Stainsby
Professor of Physiology

This dissertation was submitted to the Graduate Faculty of the College of Medicine and the the Graduate Council, and was accepted as partial fulfillment for the requirements of the degree of Doctor of Philosophy.

August, 1982

Dean, College of Medicine 7/14/82

Dean for Graduate Studies and and Research